University of Stavanger

FACULTY OF SCIENCE AND TECHNOLOGY

MASTER'S THESIS

Study program/Specialization: Industrial Economics/ Finance and Risk Management	Spring semester, 2019 Open
Authors: Dahl, Petter Holst El-Adawy, Leo	Petter H. Dahl ..... (signature of author) Leo El-Adawy ..... (signature of author)
Faculty supervisor: Dahl, Roy Endré	
Title of thesis: *"Volatility Spillover in Crude Oil Markets – a Study on Major Crude Oil Benchmarks"*	
Credits (ECTS): 30	
Key words: Crude oil prices, volatility, spillover, benchmark, world and regional market factors, Diebold and Yilmaz, generalized spillover index.	Pages: 73 + enclosures: 0 Stavanger, 12/06-2019

Acknowledgement

First of all, we would like to express our deepest gratitude to our supervisor Roy Endré Dahl for his guidance and support. His expertise and feedback have helped us during our work and have led to an improved understanding of the topic. A special thanks to Sindre Lorentzen from the Department of Industrial Economics at the University of Stavanger for sharing his expertise in time series analysis. Finally, we would like to express our gratitude to our families, for everlasting support and encouragement during our work.

Abstract

There exists a considerable body of research literature investigating the connectedness *between* crude oil markets and other financial markets. However, connectedness *within* the crude oil market has received little attention. With this in mind, the current thesis aims to highlight the research gap in literature regarding volatility spillover effects within the crude oil market. For this purpose, using daily spot prices from May 1996 to January 2019 for a set of 17 crude oils, we utilize the generalized spillover index developed in Diebold and Yilmaz (2009; 2012) to explore the connectedness within the crude oil market in terms of volatility spillovers. The generalized spillover index allows identifying the strength, as well as direction of the volatility spillovers across time. In general, our results suggest that the volatility spillover is time-varying, both in terms of strength and direction. The results further indicate that the Dubai benchmark is the most significant contributor to uncertainty in the global crude oil market, and this is especially the case after the initiation of the Arab Spring. In addition, our results suggest that the Brent benchmark behaves as a volatility buffer, reducing the uncertainty in the geographically closest regional crudes. The Dubai benchmark appears to be most affected by Middle Eastern crudes. However, our results suggest that after the Tokyo Commodity Exchange changed to Dubai as their sole underlying asset in their Crude futures contracts, the connectedness between Dubai and Asian/Australian crudes increased. As opposed to Brent, the WTI benchmark is less affected by its geographically closest crudes. These findings add important information to hedgers and speculators concerning the interdependence within the crude oil market. Further, we identify strength and direction of volatility spillover by utilizing the generalized spillover index developed in Diebold and Yilmaz (2009; 2012), and our findings are supported by market events which confirm that the methodology is well suited for this kind of analysis.

Table of Contents

Acknowledgement i
Abstract ii
Table of Contents iii
List of Figures vi
List of Tables vii
List of Abbreviations viii
1 Introduction 1
2 Crude Oil Market 4
2.1 Importance of the Crude Oil Market 4
2.2 Historical Crude Oil Pricing Systems 5
2.3 General Structure of the Petroleum Industry 6
2.4 Crude Oil Classification 6
2.5 Benchmark Crudes 8
2.6 Transportation Cost 8
2.6.1 Tanker Ships 9
2.6.2 Pipelines 9
2.6.3 Railroads 9
2.6.4 Tank Truck 10
2.7 Crude Oil Transactions 10
2.7.1 Spot Market 10
2.7.2 Futures Contracts 12
2.7.3 Contract Transactions 14
2.7.4 Summary of Crude Oil Transactions 14
2.8 Storage 14
3 Theoretical Background 17
3.1 Basics of Time Series Analysis 17
3.1.1 Time Series Data 17
3.1.2 Time Series Regression 17
3.1.3 Assumptions 20
3.1.4 Stationarity and non-stationarity 21
3.2 Vector Autoregression 22
3.2.1 The Autoregression Model 22
3.2.2 The Vector Autoregression Model 23
3.2.3 VAR model selection 24
3.2.3.1 Schwarz criterion 24
3.2.3.2 Akaike's information criterion 25

3.2.3.3 Hannan-Quinn criterion 25
3.2.3.4 Final prediction error 25
3.2.4 Other VAR Representations 26
3.2.4.1 Moving average representation 26
3.2.4.2 Companion form representation 27
3.2.5 Forecast Error Variance Decomposition 28
3.3 Descriptive Statistical Tests 28
3.3.1 Normality 28
3.3.2 Autocorrelation 29
3.3.3 Stationarity 29
3.3.3.1 Augmented Dickey-Fuller Test 30
3.3.3.2 Phillips-Perron Test 30
3.3.3.3 Dickey-Fuller General Least Squares 30
3.4 Volatility 30
3.4.1 Historical Volatility 31
3.4.2 Squared log-returns 31
3.4.3 Intraday Volatility 31
3.4.4 Volatility Spillover 31
4 Data and Methodology 33
4.1 Data 33
4.2 Methodology 38
4.2.1 Generalized Spillover Index 38
4.2.2 Deriving the Generalized Spillover Index 39
4.2.2.1 Forecast error variance decomposition 39
4.2.2.2 Generalized total spillover index 40
4.2.2.3 Generalized directional spillovers and net spillovers 41
4.2.2.4 Generalized net pairwise spillovers 41
4.2.3 The Generalized Spillover Index in R 41
4.2.3.1 Construction of a VAR model 42
4.2.3.2 Computing the forecast error variance decomposition table 42
4.2.3.3 Full-sample analysis and rolling-window analysis 43
5 Empirical results 45
5.1 Analysis of Crude Oil Benchmarks 46
5.1.1 Full-Sample Analysis of Volatility Spillover 46
5.1.2 Rolling-Window Analysis of Volatility Spillover 48
5.2 Analysis of Brent and Regionals 54
5.2.1 Full-Sample Analysis of Volatility Spillover 54

5.2.2 Rolling-Window Analysis of Volatility Spillover 55
5.3 Analysis of Dubai and Regionals 58
5.3.1 Full-Sample Analysis of Volatility Spillover 58
5.3.2 Rolling-Window Analysis of Volatility Spillover 59
5.4 Analysis of WTI and Regionals 61
5.4.1 Full-Sample Analysis of Volatility Spillover 61
5.4.2 Rolling-Window Analysis of Volatility Spillover 62
6 Conclusion 66
7 References 68

List of Figures

Figure 1: Historical benchmark prices from 1996 to 2019. 11
Figure 2: Illustration of futures term-structure, contango and backwardation. 13
Figure 3: Weekly U.S. Ending Inventory of Crude Oil (Million Barrels) 16
Figure 4: Total volatility spillover index for crude oil benchmarks. 49
Figure 5: EIA estimates of U.S. oil production per region 51
Figure 6: Net pairwise volatility spillovers between benchmark crudes. 52
Figure 7: Volatility spillover from benchmark crudes TO others. 53
Figure 8: Total volatility spillover index for Brent and regionals. 56
Figure 9: Net pairwise volatility spillovers between Brent and regionals. 57
Figure 10: Total volatility spillover index for Dubai and regionals. 60
Figure 11: Aggregated net pairwise volatility spillovers between Dubai and regionals. 61
Figure 12: Total volatility spillover index for WTI and regionals. 63
Figure 13: Price spread between WTI and LLS during the U.S. shale oil revolution. 64
Figure 14: Net pairwise volatility spillovers between WTI and regionals. 65

List of Tables

Table 1: Classification of crude oil based on API gravity 7
Table 2: Characteristics of benchmark crudes. 8
Table 3: Field location, API gravity, sulfur content and total acid number for benchmark and regional crudes. 34
Table 4: Descriptive statistics of price data. 35
Table 5: Descriptive statistics of daily log-returns (%). 36
Table 6: Descriptive statistics of daily volatility (%). 37
Table 7: Descriptive statistical tests for the daily volatilities of the price series. 38
Table 8: Illustration of a FEVD table. 40
Table 9: VAR model selection; SC, AIC, HQ and FPE for all analyses. 46
Table 10: Volatility spillover table for all benchmarks (Brent, Dubai and WTI). 47
Table 11: Net pairwise spillover table for all benchmarks (Brent, Dubai and WTI). 47
Table 12: Volatility spillover table for Brent and regionals. 54
Table 13: Net pairwise spillover table for Brent and regionals. 55
Table 14: Volatility spillover table for Dubai and regionals. 58
Table 15: Net pairwise spillover table for Dubai and regionals. 59
Table 16: Volatility spillover table for WTI and regionals. 62
Table 17: Net pairwise spillover table for WTI and regionals. 62

List of Abbreviations

The following abbreviations are used in the thesis:

Abbreviations		Full forms
ADF	-	Augmented Dickey-Fuller
AIC	-	Akaike`s information criterion
AR	-	Autoregression
BIC	-	Bayesian information criterion
CLT	-	Central limit theorem
DF	-	Dickey-Fuller
DF-GLS	-	Dickey-Fuller general least squares
E&P	-	Exploration and production
FEVD	-	Forecast error variance decomposition
FPE	-	Final prediction error
GLS	-	General least squares
GSP	-	Government selling price
HQ	-	Hannan-Quinn
ICE	-	Intercontinental Exchange
i.i.d.	-	Independently and identically distributed
JB	-	Jarque-Bera
KPPS	-	Koop, Potter, Pesaran and Shin
KPSS	-	Kwiatkowski, Phillips, Schmidt and Shin
LLN	-	Law of large numbers
LLS	-	Louisiana Light Sweet
LM	-	Lagrange multiplier
MA	-	Moving average
MLE	-	Maximum likelihood estimation
MSFE	-	Mean squared forecast error
NYMEX	-	New York Mercantile Exchange
NWA	-	North West Australian
OLS	-	Ordinary least squares
OPEC	-	Organization of the Petroleum Exporting Countries
OSP	-	Official selling price
PM	-	Portmanteau
PP	-	Phillips-Perron
RMSFE	-	Root mean squared forecast error
SC	-	Schwarz criterion
SSR	-	Sum of squared residuals
TAN	-	Total acid number
TOCOM	-	Tokyo Commodity Exchange
U.S.	-	United States
VAR	-	Vector autoregression
WTI	-	West Texas Intermediate
WTS	-	West Texas Sour

1 Introduction

Crude oil is often thought of as a single uniform commodity. However, the global crude oil market contains several crude oils produced at numerous locations and with different quality and characteristics. Due to this diversity, major benchmarks such as Brent, WTI and Dubai are used to provide a standard for regional crudes with similar characteristics and quality as their closest benchmark. With this in mind, density, sulfur content as well as acidity are important characteristics for buyers of crudes, and when considered in conjunction with transportation cost, they provide helpful guidelines for pricing the diverse commodity.

The crude oil market is well-known to be complex, and the oil price is affected by several uncertain determinants such as global oil supply and demand, inventories, OPEC decisions, financial crises, national elections and geopolitical unrest (Wei et al., 2017). As one of the biggest commodity markets in the world, historical oil prices are characterized by high fluctuations, occasional jumps exceeding the normal fluctuations, and a tendency to revert to a long-term mean (Begg and Smit, 2007). A common method to analyze the degree of uncertainty in crude oil prices is to utilize the concept of volatility. In general terms, volatility is a measure of the size of the fluctuations in a time series.

Crude oil prices are experiencing high levels of volatility (Pindyck, 2004b), and this brings more risk to the decision-making process for investors, speculators, hedgers and policy makers that are depending on crude oil prices (Zavadska et al., 2018). For instance, crude oil benchmarks are often studied in conjunction with other financial assets such as equities, commodities, bonds and currencies. As the crude oil markets play a vital role in the world economy, a significant amount of research studies have been conducted to analyze the interactions between the crude oil market and other financial markets (e.g. Kilian and Park, 2009; Pindyck, 2004b; Breitenfellner and Cuaresma, 2008; Ciner et al., 2013).

Across time, the volatility within a market may be affected by volatilities of other financial markets, and such cross-market volatilities are commonly referred to as volatility spillovers (Ke et al., 2010). The volatility spillover between markets may be time-varying in terms of intensity and direction, and it can provide early signals of potential crises (Diebold and Yilmaz, 2012). There exists a considerable body of literature analyzing the interdependence between the crude oil market and other financial markets in terms of volatility spillovers. For instance, Arouri et al. (2011), Awartani and Maghyereh (2013) and Malik and Hammoudeh (2007) explore the volatility spillovers between crude oil and equity markets, and they conclude that significant

spillover exists between crude oil and equity markets. Furthermore, Du et al. (2011), Baruník et al. (2015) and Nazlioglu et al. (2013) find significant spillover between crude oil and commodity markets such as corn, wheat, soybean, heating oil and gasoline. Finally, the volatility spillover between crude oil markets, bonds and currencies are reviewed by e.g. Baek and Seo (2015) and Singh et al. (2019), and they find significant volatility spillover for crude oil against bond and currency markets, respectively.

Previous research has primarily focused on the spillover *between* crude oil markets and other markets. Despite the amount of research on this area, a lack of insight related to volatility spillover *within* the crude oil market exists. This research gap forms the point of departure for this thesis. To shed light on this research gap, we perform an analysis of the volatility spillover within the crude oil market by utilizing the generalized spillover index developed in Diebold and Yilmaz (2009; 2012). According to Kang et al. (2017), this is the only method allowing for estimation of directional and net spillover in addition to total spillover. This is advantageous as it allows for identification of both main transmitters and receivers of price uncertainty in the global crude oil market. Thus, Diebold and Yilmaz´s generalized spillover index has proven beneficial in previous discussions on volatility spillovers (e.g. Zhang, 2017; Ji et al., 2018; Husain et al., 2019). Therefore:

> *The objective of the current thesis is to explore volatility spillover between a set of crude oil prices by means of the generalized spillover index developed by Diebold and Yilmaz.*

With this objective as a specified course of action, the work of this thesis aims to add new knowledge about interdependence within the crude oil market. First, we consider the connectedness between the three major benchmarks Brent, Dubai and WTI. Second, we perform separate analyses of the connectedness for each major benchmark against minor regional crudes based on their geographic distance to their closest benchmark. As already described, the oil market is complex. Thus, we will interpret the results in light of typical determinants affecting crude oil prices over time, such as global oil supply and demand, inventories, OPEC decisions, financial crises, national elections and geopolitical unrest.

The thesis is organized as follows. Chapter 2 gives a brief introduction to the structure of the crude oil market, including information about the importance of the crude oil market, pricing systems, general structure, classification of crude oils, benchmark crudes, transportation costs, transactions and the concept of storage. Chapter 3 explains the theoretical background of the

methodology utilized in this thesis. The chapter introduces general time series analysis as well as vector autoregressions. More specifically, basics about the construction of a vector autoregressive model and forecast error variance decomposition are explained. Lastly, the chapter includes a description to the concept of volatility and volatility spillover, as well as information about descriptive statistical tests for normality, autocorrelation and stationarity. This chapter, in conjunction with chapter 2, will give a firm understanding of the following chapters. Chapter 4 introduces the data for the benchmark and regional crude oil prices, as well as the methodology utilized in this thesis to estimate the volatility spillover between the crude oil markets. Chapter 5 presents the empirical results and discussion of the analyses, and finally, chapter 6 provides the conclusion of the analyses.

2 Crude Oil Market

This chapter gives a brief introduction to the crude oil market, starting with a short description of the importance of the crude oil market to the global economy and activity. In order to understand the current pricing system, a brief introduction to historical pricing systems is given as well as information about the general market structure of the petroleum industry. As crude oil is a heterogenous commodity, the many crude oils of the world are sold at different prices. Therefore, information about crude oil classification, benchmark crudes and transportation cost are provided in this chapter. Finally, the current pricing system is described in terms of three different platforms (spot market, futures contracts and contract transactions) and storage including its strategic value.

2.1 Importance of the Crude Oil Market

The crude oil market plays a vital role in the world economy and is often blamed for causing excess volatility in several asset classes such as equities, other commodities, bonds and currencies (Singh et al., 2019). Following a study by Kilian and Park (2009), the underlying supply and demand shocks causing oil price fluctuations account for about 20% of the long-term variation in the United States (U.S.) stock returns. Historical oil crises have shown ripple effects across industries, in particular such crises caused concerns about both price and availability of energy resulting in postponement of investment decisions (Hamilton, 1996). A study by Phan et al. (2018) on the relationship between oil price uncertainty and corporate investments concludes that there exists a negative relationship, and that this effect is more comprehensive in oil producing countries and companies. Furthermore, a study on the relationship between oil price shocks and unemployment rate in Europe conducted by Cuestas and Gil-Alana (2018) concludes that the oil price and unemployment rate move in the opposite direction. The authors further specify that the magnitude of the effect is greater for negative price shocks, than for positive.

Crude oil interests have caused severe events such as financial crises, and geopolitical unrest such as civil wars and regime falls throughout history. For example, a study by Hamilton (1983) reveals a significant relationship between dramatic crude oil price increases and subsequent U.S. recessions. However, according to Kilian and Vigfusson (2017) not all dramatic crude oil price increases were followed by a recession in the U.S. Another study shows that the initiation of civil wars seems to be linked to the country's level of oil dependence (Ross, 2004), especially for oil exporting countries with onshore production (Basedau and Richter, 2014). For instance, oil played a direct role in the initiation of civil wars in Angola, Indonesia, Iran and Nigeria (Le

Billon, 2001; Rustad and Binningsbø, 2012). It is also speculated that the collapse of Saddam Hussein's regime was partly initiated by U.S. oil interests in Iraq (Jhaveri, 2004). Furthermore, the trienio government in Venezuela, and the Mossadegh regime in Iran have both been subject to military coups directly related to oil conflicts (Karl, 1997; Kinzer, 2008).

On the other hand, financial crises and geopolitical events have also caused increased uncertainty in the crude oil market. For instance, Hamilton (2011) suggests that the financial stress during the East Asian crisis of 1997-98 caused a drop in oil price because the oil consumption in these countries decreased. Furthermore, Hamilton (2003) states that the East Asian crisis of 1997-98 was associated with a 50% drop in oil price. In terms of geopolitical unrest, Bhar et al. (2008) conclude that the volatility in benchmark crudes such as Brent, Dubai and WTI increases during times of geopolitical unrest in the Middle East. Moreover, Baumeister and Kilian (2016a) state that geopolitical unrest such as during the Arab Spring causes uncertainty about future scarcity of oil. This increased uncertainty may cause the oil price to shift.

2.2 Historical Crude Oil Pricing Systems

In order to understand the current pricing system in the market, it is crucial to have a firm understanding of the previous pricing systems and their corresponding price concept. Until the late 1950s, the oil industry was primarily dominated by a few large multinational oil companies, commonly referred to as the Seven Sisters[1]. The governments controlling the petroleum resources did not participate in production, nor pricing, of the crude oils. Until the mid-1970s, the pricing system was based on the concept of posted price. The posted price acted as a parameter to calculate the income tax accruing to host governments for selling oil concessions. However, the Seven Sisters experienced increased competition from independent oil companies during the 1960s. This, and the fact that OPEC (Organization of the Petroleum Exporting Countries) countries stopped granting new concessions, as well as claiming equity participation in the current concessions, gave rise to new pricing concepts such as official selling price (OSP) and government selling price (GSP). Due to increased equity participation from the multinational oil companies, OPEC countries were given a share of the oil production in which they sold to third party buyers at OSP and GSP. This oil was often sold back to the oil companies that held the concessions at a buyback price. Hence, in the early 1970s, the oil pricing system

[1] The Seven Sisters comprise of the following multinational oil companies; Standard Oil of New Jersey (ESSO), Standard Oil Company of New York (Socony), Standard Oil of California (Socal), Gulf Oil, Texaco, Royal Dutch Shell and Anglo-Persian Oil Company (Hilyard, 2012). These oil companies controlled 85% of the global crude oil production outside USA, China, Russia and Canada (Fattouh, 2011).

was based on (1) the posted price, (2) the OSP and GSP and (3) the buyback price. Due to its complexity, this pricing system lasted no longer than to 1975. The new pricing system that emerged after the buyback system, was entirely based on price determination by OPEC. The concept was based on benchmark pricing, meaning that OSP and GSP were set at either a discount or a premium relative to the chosen benchmark. During the mid-1980s, the OPEC driven pricing system collapsed with the increase of oil produced by non-OPEC countries and the current market related pricing system emerged in 1986. In other words, the price determination power changed from OPEC to the global market (Fattouh, 2011; Fattouh, 2006).

However, OPEC still plays a significant role in the current pricing system. A study conducted by Kaufmann et al. (2004) indicates that OPEC has a substantial effect on the oil price through their decision activities concerning quotas, production level and operable capacity. Furthermore, Schmidbauer and Rösch (2012) suggest that OPEC decisions are associated with changes in oil price volatility. The authors further state that the extent of the volatility changes associated with OPEC decisions are depending on the type of decision, and that decisions to cut or maintain current production level have a greater impact compared to a decision to increase the production level.

2.3 General Structure of the Petroleum Industry

In general terms, the oil and gas industry is divided into three segments; (1) upstream (exploration and production (E&P)), (2) midstream (transportation and trading) and (3) downstream (refining and marketing) (Inkpen and Moffett, 2011). Oil companies that desire more control throughout the value chain are integrating themselves into one additional segment or all market segments. If an oil company is operating in upstream, midstream and downstream, it is said to be a fully integrated oil company (Chima and Hills, 2007). Examples of such companies include Equinor (Equinor, 2019), BP (BP, 2019), Shell (Shell, 2019), Chevron (Chevron, 2019) and Total (Total, 2019).

2.4 Crude Oil Classification

As the crude oil market contains several crudes, the petroleum industry often classifies the different crudes according to three main parameters; (1) geographic location, (2) API gravity and (3) sulfur content. The first parameter, geographic location, refers to the location in which the crude oil is produced. It is a crucial parameter as it affects the cost of transportation from site to a petroleum refinery (Hilyard, 2012). The second parameter, API gravity, is the preferred property for measuring crude oil density. The API gravity is calculated directly from the

specific gravity of the crude oil, which is the density of the crude oil relative to pure water (Speight, 2017).

$$API = \frac{141.5}{Specific\ gravity} - 131.5 \quad (2.1)$$

Fahim et al. (2009) present a scheme for classification of crudes according to API gravity (Table 1):

Table 1: Classification of crude oil based on API gravity (Based on Fahim et al., 2009).

Crude category	**API gravity**
Light	API > 38
Medium	29 < API < 38
Heavy	8.5 < API < 29
Very heavy	API < 8.5

It is important to keep in mind that API gravity alone does not classify the crude oil adequately (Speight, 2017). As seen in equation (2.1) the API gravity is inverse proportional to the crude oil density. This means that the lighter the crude oil, the higher the API gravity. The refinery process of a light crude oil will generally yield products such as gasoline, jet fuel and diesel. These are products with increasing demand. Heavy crude oils can be processed into heavier products such as industrial fuels and asphalt, or they can be further processed into smaller compounds to yield other fuels (Demirbas et al., 2015). Due to the refinery process, light crudes are more valuable than heavy crudes because they yield more valuable products (McKinsey, 2019). The third parameter for classifying crudes, sulfur content, is the most important factor for crude oil refineries. This is mainly because it is poisonous and can cause corrosion of the refinery equipment. The sulfur content is commonly measured as the weight percentage of sulfur in the crude (Demirbas et al., 2015). A crude oil is called sweet when it contains low levels of sulfur, and sour when it contains high levels of sulfur (Hilyard, 2012). When crudes with high sulfur content are burned, high levels of sulfur-dioxide are produced and this consequently leads to acidic depositions (Speight, 2015). Thus, a sweet crude does in general trade at a premium compared to a sour crude (Inkpen and Moffett, 2011).

Bacon and Tordo (2005) suggest including another parameter for classifying crudes, namely total acid number (TAN). TAN is a measure of the acidity of the crudes. The industry shows a growing interest for this parameter because the production of high acid crudes is increasing. Similar to negative features of high sulfur content, a high acidic crude will cause corrosion of

refinery equipment (Speight, 2015). TAN is measured as the amount of potassium hydroxide needed to neutralize one gram of the sampled crude oil, mg KOH/g. TAN works as an accepted measure of the crude oils potential corrosive abilities (Bacon and Tordo, 2005).

2.5 Benchmark Crudes

As discussed in subchapter 2.4, crudes vary significantly in quality. When a commodity, such as crude oil, is heterogenous it is often useful to establish benchmarks (Van Vactor, 2010). Benchmark crudes are oil produced from an area where its molecular characteristics have been determined in order to be used as a pricing reference in the global crude oil market (Hilyard, 2012). This is advantageous to global buyers and sellers as they can price the regional crudes at either a discount or a premium relative to a particular benchmark crude (Fattouh, 2010). The price differentials are mainly determined by the difference in transportation cost, quality, as well as taxes for the crudes that are compared. Some common benchmark crudes include Brent, Dubai and West Texas Intermediate (WTI). Brent is a light sweet crude oil and is made up of 15 crudes mainly from the North Sea. Brent is used as a benchmark for oil production in Europe and Africa, as well as oil imports from the Middle East flowing to the west (Hilyard, 2012). Dubai is a medium sour crude oil, and is used as a benchmark for Middle East crudes flowing to the Asian-Pacific market (Fattouh, 2006). WTI is a light sweet crude oil of high quality (Hilyard, 2012), and is the main benchmark used for pricing oil produced in, and imported to, the U.S. (Fattouh, 2006). Table 2 summarizes the API gravity, sulfur content and TAN for the abovementioned benchmark crudes:

Table 2: Characteristics of benchmark crudes.

	Field location	**API gravity**	**Sulfur content**	**Total acid number**
Brent	UK	37.5°	0.40%	0.03
Dubai	UAE	31.4°	1.96%	0.25
WTI	US	40.6°	0.22%	0.10

2.6 Transportation Cost

The transportation costs in the petroleum industry are associated with the shipment of oil from one party to another, often transported by tanker ships, pipelines, railroads or tank trucks. Some major E&P companies own transportation equipment themselves, and some acquire these services from independent transportation operators (Hilyard, 2012). In terms of barrels-per-kilometer, tanker ships are cheapest, with pipelines second, railroads third and tank trucks being the most expensive (Abdel-Aal and Alsahlawi, 2013). The location of production is of great

importance, because the closer the production site is to major refinery markets, the cheaper the transportation cost. Therefore, oil produced near refineries will trade at a premium relative to oil produced far from refineries (Bacon and Tordo, 2005). A key thing to remember is that the transportation cost is affected by the characteristics of the crude itself. A crude with a TAN greater than 1 is considered corrosive by the petroleum industry, and those crudes will trade at a discount relative to others, partly because it requires more robust transportation equipment (Abdel-Aal and Alsahlawi, 2013; Bacon and Tordo, 2005). Similarly, a sour crude (crude with high sulfur content) will cause sulfur corrosion on the transportation equipment (Wang et al., 2003), and hence increase the maintenance and operation costs (Meriem-Benziane et al., 2017).

2.6.1 Tanker Ships

Tanker ships are the most important transportation method, and accounts for nearly 40% of the global fleet. This is due to the fact that the world's main oil producers do not have any land connections in terms of rigid transportation equipment (such as pipelines), and are far away from their natural market (Abdel-Aal and Alsahlawi, 2013).

2.6.2 Pipelines

Transporting crudes via pipeline systems are more complex than tanker ships, for the reason that it is a rigid system only transporting through a limited number of routes. Pipelines introduce excess uncertainty to the oil price as they cross national borders and are therefore subject to strategic and political problems. For instance, countries can choose to change transit fees or even cut off the entire supply. For example, in 2009 Russia decided to cut off the gas supply to Europe in an attempt to change the entire pricing system of petroleum supply to Europe (Abdel-Aal and Alsahlawi, 2013). Heavy crudes (low API) are more difficult to transport via pipelines as conventional pipeline technology are mainly developed for light crudes (high API). Transporting heavy crudes requires either a high-pressure pipeline system, or decreasing the viscosity of the crude by solvents, both in which are expensive (Martínez-Palou et al., 2011). According to Meriem-Benziane et al. (2017), high sulfur content leads to corrosion of the inner wall of the pipeline system which again increases maintenance cost. In general, sour crudes trade at a discount relative to sweet crudes, and this is partly because of the corrosive effect on transportation equipment and other equipment in the value chain (Fattouh, 2011).

2.6.3 Railroads

Before the pipeline systems were introduced to the global petroleum transportation system, railroads were the most important method. Railroads are important in today's market as it provides a cheaper alternative than tank trucks when transporting on land. This is mainly

because railroad tanks can transport a greater amount of petroleum per vehicle (Abdel-Aal and Alsahlawi, 2013). However, railroads are not capable of transporting the same amount of oil as pipelines (Kilian, 2016)

2.6.4 Tank Truck

Tank trucks prove useful in today's market for local transportation as it is a more flexible method than the other land-based transportation methods. Furthermore, tank trucks are used when the cost of implementing a pipeline system cannot be justified. This often occurs for small facilities, where small amounts of crudes are produced (Abdel-Aal and Alsahlawi, 2013).

2.7 Crude Oil Transactions

The crude oil transactions occur on three different platforms, namely (1) spot market, (2) futures contracts and (3) contract transactions (Inkpen and Moffett, 2011).

2.7.1 Spot Market

Generally, a spot market is a market where products are sold and delivered simultaneously. Moreover, for crudes a spot transaction is an agreement to sell or buy a shipment of crude oil at an agreed upon price. Due to the nature of the crude oil market, spot contracts often include delivery within a month. For both producers and refiners of crudes, the spot market has a balancing effect of supply and demand (Inkpen and Moffett, 2011). For instance, if a company currently has a greater supply than needed it can sell the excess crudes on the spot market to the highest bidder willing to take delivery of the shipment (Hilyard, 2012). To that end, the prices of the crudes in the spot market reflect the current balance between supply and demand. For example, an upward trending spot price indicates that an increase in supply is needed, and a downward trending spot price indicates the opposite. The price of crudes in the spot market is subject to events such as natural disasters, political turbulence, severe weather, as well as changes in supply and demand (Hilyard, 2012).

Spot prices are reported for transactions in many different regional markets, including North-West Europe, New York Harbor and South East Asia (Inkpen and Moffett, 2011). Fattouh (2006) suggests that the spot market for benchmark crudes is flawed. The author highlights three reasons, (1) less trading of the benchmarks occurs, (2) the characteristics of an average barrel sold are no longer close to the benchmark specifications and (3) Fattouh argues that the spot market for Brent no longer exists.

Figure 1 illustrates the historical oil price from May 1996 to January 2019 for the three benchmarks Brent, Dubai and WTI. Prices are extracted from Thomson Reuters Eikon[2].

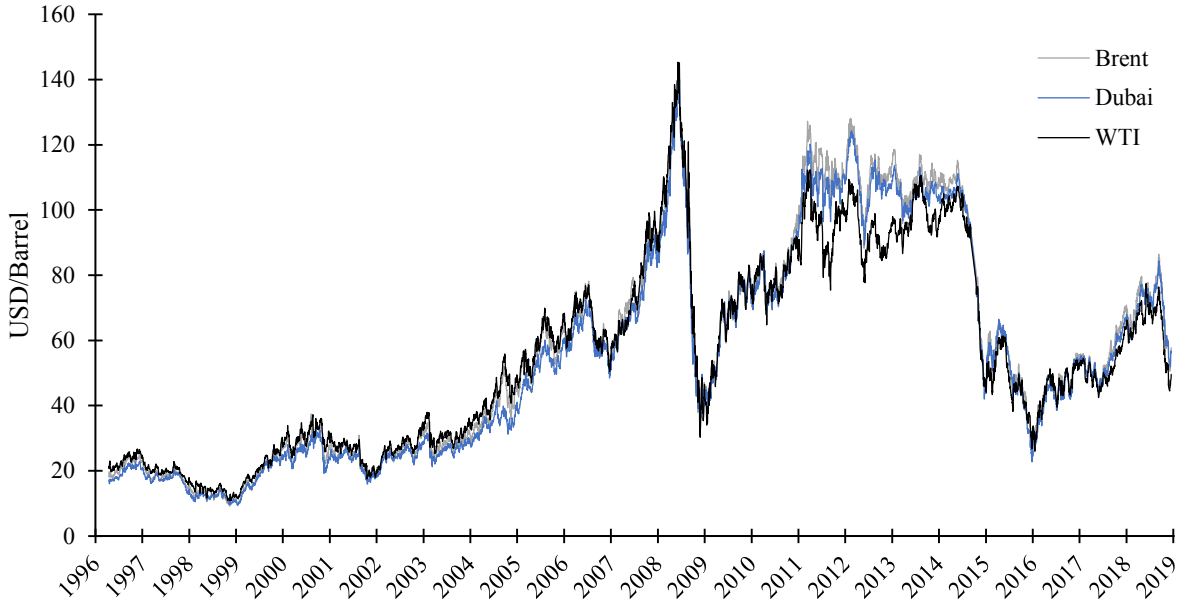

Figure 1: Historical benchmark prices from 1996 to 2019.

It is evident from Figure 1 that oil prices are volatile, and the recognized instability of crude oil prices has led to the development of a futures market for crude oils (Albinali and Dahl, 2014). According to Baumeister and Peersman (2013), the price inelasticity of crude oil supply and demand cause high volatility in the crude oil market. The authors further state that even small disturbances on either the supply or demand side of the crude oil market may cause large shifts in the oil price. For instance, the rapid increase in U.S. oil production at the beginning of the U.S. shale oil revolution caused downward pressure on the WTI benchmark due to excess supply in the market (Kilian, 2016).

The relatively steep oil price increase lasting from 2003 until 2008 was primarily caused by rising global demand for industrial commodities due to an unexpected growth in the global economy. In particular, growth in emerging economies such as China, Russia and Japan were unexpected by the markets (Kilian and Hicks, 2013). The price shock that occurred during the last quarter of 2007 until the end of first half of 2008 is one of the largest oil price shocks experienced throughout history (Hamilton, 2008). Hamilton (2009) highlights three factors causing this price shock. First, the author points out the growing global crude oil demand, especially in China. Notably, from 2005 to 2007 the Chinese daily consumption of oil increased

[2] Thomson Reuters Eikon is an analysis and trading software that distributes a wide variety of market data including commodity prices, equities pricing data etc.

by 870,000 barrels. Second, the oil supply failed to increase during the same period, and it stagnated. Increasing global demand coupled with stagnated oil supply caused a significant increase in oil price to sufficiently reduce the global oil consumption. Third, the rapid oil price increase was further exacerbated by speculators. With the increasing oil price, the pressure on the long side of the futures contracts increased, which again resulted in an increasing futures price. Consequently, the oil price in the spot market followed and this further resulted in a speculative bubble. The bubble popped in mid-2008 causing a subsequent oil price collapse (Hamilton, 2009).

2.7.2 Futures Contracts

A futures contract is a promise to deliver or receive a standardized quantity and quality of a commodity, or financial instrument, at a specified location, price and time in the future (Schwager and Etzkorn, 2017). The futures market consists of both hedgers and speculators. Hedgers want to reduce price risk (risk associated with unexpected changes in price) via the activity of hedging, whereas speculators want to bear price risk in expectation of earning a profit. Hence, a futures contract provides a mechanism for hedging against spot price volatility. However, the activity of hedging not only reduces price risk, but it can also be profitable for the hedger if the contracted price exceeds the corresponding costs. Futures contracts are traded on a futures exchange. The futures exchange finds a party willing to sell a futures contract, as well as a party willing to buy the same contract. These parties are obliged to make, and take delivery of the contracted crude, respectively (Tomek and Kaiser, 2014). However, the main purpose of a futures contract is not to provide a mechanism for actual delivery, but rather allowing market participants to spread risks to those willing to bear it (Fattouh, 2006). According to Pindyck (2001), most of the futures contracts are rolled over and never result in actual delivery.

The futures prices include information about the market's expectations about future intersections of demand and supply, and hence they reflect the expected future spot price. The concept of futures term-structure reveals important information about the market's expectation about future crude prices. The term-structure is obtained by plotting the current spot price P_t along with futures prices in order of increasing maturity, $F_{t|t+1}, F_{t|t+2}, \dots, F_{t|T}$. Figure 2 illustrates two scenarios, (1) contango and (2) backwardation. Contango is when the market expects future spot prices to increase relative to the current spot price, while backwardation is the opposite (Øglend, 2018).

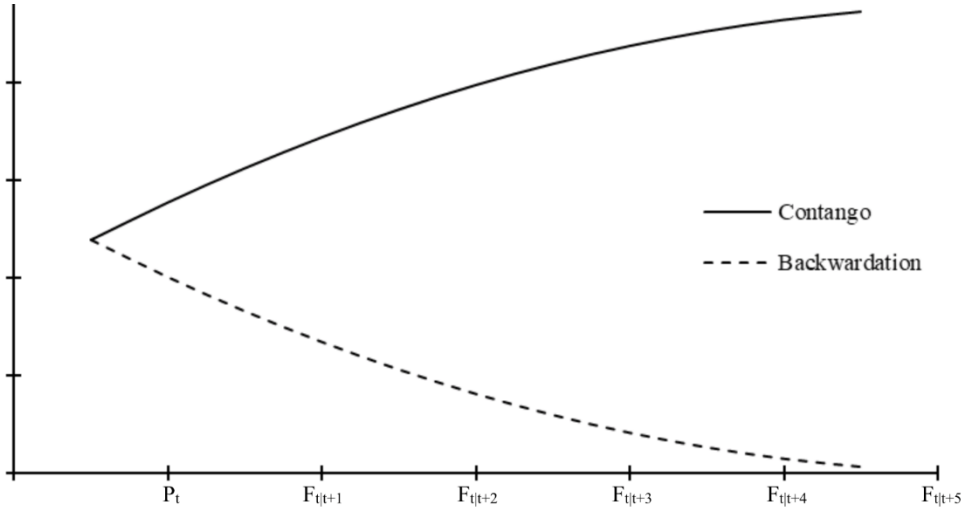

Figure 2: Illustration of futures term-structure, contango and backwardation.

The pricing of futures contracts is based on benchmark pricing, which again is based on the spot price. The benchmark oil prices are determined at the end of each business day based on information from (1) oil trade journals assessing spot prices among other factors and (2) the exchanges. Important exchanges for trading crude oil futures include New York Mercantile Exchange (NYMEX), the Intercontinental Exchange (ICE) and Tokyo Commodity Exchange (TOCOM). The WTI futures contracts have been traded on NYMEX since 1983 and the standardized contract is an agreement to deliver 1000 barrels of WTI at Cushing, Oklahoma. Similarly, the ICE Brent futures contract is traded on ICE (Fattouh, 2006). The price of a futures contract is built on an underlying asset, which for the crude oil market often is a benchmark crude. The strategy for hedgers that want to eliminate price risk, is then to find a futures contract with an underlying asset that closely correlates with the spot price of the asset in question. A low correlation between the underlying asset in the futures contract and the asset the hedger holds, will reduce the effectiveness of the hedging activity (Øglend, 2018).

Whilst a futures contract protects a producer from both upside and downside risk, producers can buy option contracts to avoid downside risk and still retain upside risk. However, an option contract is not free to enter like a futures contract. Buying an option contract gives the buyer the right to either sell, or buy a futures contract at a specified futures price, commonly referred to as the strike price (Tomek and Kaiser, 2014). A popular approach to determine the price of an option contract is to use the Black-Scholes method (Rad et al., 2018). This method requires the following five input parameters; the asset price, the strike price, the exercise date, the risk-free rate and the volatility. Note that the only parameter that needs to be estimated is the volatility, all the other parameters are observable in the market (Berk and DeMarzo, 2007). As

stated in Poon and Granger (2005) the most important parameter in determining the option price with the Black-Scholes model is the volatility. The authors further state that by observing the option prices traded in the market, it is possible to infer how the market view the future volatility (Poon and Granger, 2005).

Finally, if delivery of the contracted crude is necessary, Cushing, Oklahoma, acts as a delivery point for the futures contracts traded on NYMEX. This delivery point is commonly referred to as a hub. Hubs are the point where oil transporting pipelines come together and are often referred to as gathering stations. Much of the crude oil price discovery is associated with hubs. Important hub locations worldwide for price discovery include Cushing, ARA (Amsterdam, Rotterdam and Antwerp) and the Arab Gulf (Hilyard, 2012).

2.7.3 Contract Transactions

Oil E&P companies must find customers willing to buy their produced oil, and crude oil is usually sold and delivered via contract transactions (Inkpen and Moffett, 2011). These contractual arrangements involve buyer and seller agreements concerning type of product to be delivered, location of delivery, quantity, quality and price (Van Vactor, 2010). As opposed to futures contracts, contract transactions actually result in a customer taking delivery of the produced crude oil. The main customer taking delivery of the oil produced by E&P companies are refineries, who further process the crudes into more commercial products. Both the spot market and futures contracts provide crucial pricing information for such contractual agreements for crude oil transactions. Crude oil trading is often conducted by the E&P company itself, but also by specialist firms (Inkpen and Moffett, 2011).

2.7.4 Summary of Crude Oil Transactions

The crude oil transactions occur on three different platforms, (1) spot market, (2) futures contracts and (3) contract transactions. Firstly, the spot market yields information about current supply and demand. Secondly, the futures contracts reflect the markets expectations about future crude oil prices. Finally, contract transactions are arrangements where the oil is actually sold and delivered (Inkpen and Moffett, 2011).

2.8 Storage

In a competitive commodity market with high volatility on both the supply and demand side, the features of storage prove useful for both produces and consumers, as well as for speculators. For instance, producers can hold inventories in order to reduce costs associated with variations in production over time. Producers can choose to sell out inventory in periods of high demand,

whilst refilling the inventories during periods of low demand. This mechanism means that the production in each period does not necessarily need to equal the consumption, as oil inventories can be carried through time (Pindyck, 2001). This feature of carrying inventories tends to smooth production over time (Pindyck, 1990).

According to the theory of storage, the relationship between spot- and futures prices reveal important information for decision makers in the oil and gas market. For example, when oil prices are in contango it may be profitable to store oil and enter into a futures contract instead of selling the oil in the spot market (Jafarizadeh and Bratvold, 2013). As the example suggests, storage has the ability of carrying crude oil into the future, making crude oil a capital asset which gives the option of storing it now to create future income. The fundamental intertemporal pricing condition aids decision makers on whether to store crude oil for the future, or sell in the spot market today:

$$E_t(P_{t+1}) - P_t = rP_t + (1+r)M. \tag{2.2}$$

Equation (2.2) suggests that in equilibrium the expected price increase of one unit, $E_t(P_{t+1}) - P_t$, must compensate for both lost interest for not selling today, rP_t, and the marginal cost of storage, $(1+r)M$, often referred to as the *cost-of-carry*. Where $(1+r)$ indicates the loss of interest for paying storage fees rather than investing in something else, and *M* is the cost of storing one extra unit. When the interest rate or the marginal cost of storage increases, the expected price increase must be greater for decision makers to store. Importantly, a key feature of storage is that it has the ability to reduce the price volatility of the market in question. For instance, if information suggesting a future rise in demand reaches the market, decision makers will increase their expected future price. Hence, more commodities will be stored and consequently the current price will increase in anticipation of a future change in demand and supply (Tomek and Kaiser, 2014). According to Du et al. (2011), the volatility reducing effect of storage appears to be true for the crude oil market as well. Thus, an increase in oil price volatility will lead to crude inventory build-ups, and a subsequent oil price increase in the short-run. Consequently, increasing demand for storage will increase the marginal cost of storing one more unit of crude oil (Pindyck, 2004a).

The inventory levels are of great importance, as they represent both the supply and demand conditions of the crude oil market. However, a study by Bu (2014) reveals that it is the unexpected changes in inventory levels rather than actual changes that affect the crude oil price.

Bu further states that the unexpected changes may contain new information about demand and supply in the market, and hence causes a price shift.

Figure 3 illustrates the U.S. historical crude oil inventory from October 1982 until February 2019. The inventory data are collected from EIA (2019)[3], and they are reported on a weekly basis. A study conducted by Geman and Ohana (2009), concludes that there exists a significant negative relationship between the U.S. inventory of crude oil and the price volatility in the crude oil spot market. This indicates that a decreasing inventory level will increase the price volatility and hence the uncertainty of the future oil price.

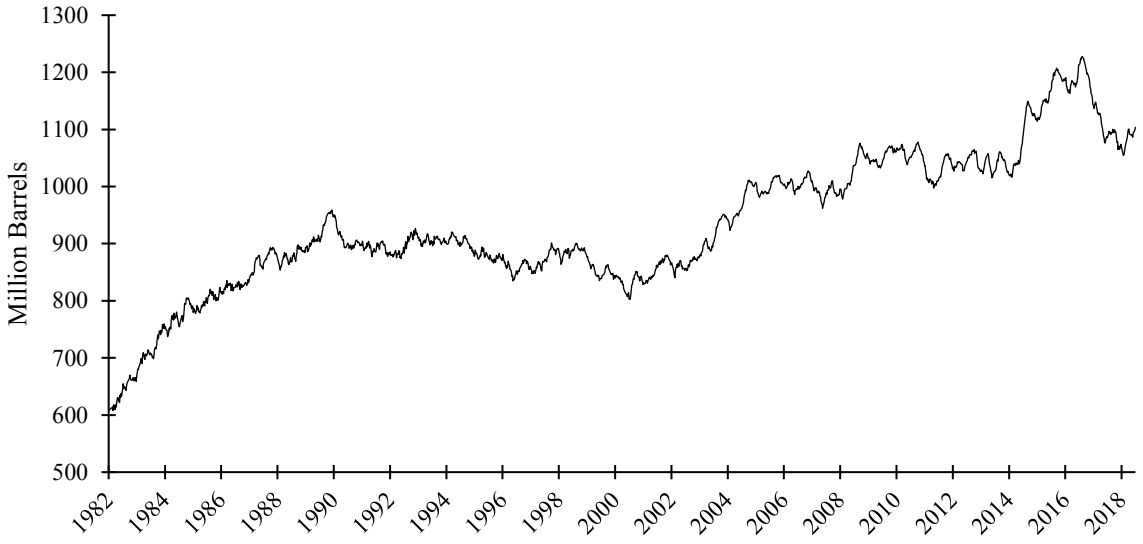

Figure 3: Weekly U.S. Ending Inventory of Crude Oil (Million Barrels) (EIA, 2019).

[3] EIA is the U.S. Energy Information Administration.

3 Theoretical Background

As previously mentioned, the generalized spillover index developed in Diebold and Yilmaz (2009; 2012) is utilized in the current thesis to assess the volatility spillover between a set of crude oil prices. In order to obtain a firm understanding of this method, the following chapter describes theory in which the methodology is based upon. For this purpose, the first part of this chapter introduces the basics of time series analysis. Furthermore, the second part introduces the concept of vector autoregression as well as forecast error variance decomposition and volatility spillover. Lastly, a brief description of statistical tests for normality, autocorrelation and stationarity is given.

3.1 Basics of Time Series Analysis

The generalized spillover index developed in Diebold and Yilmaz (2009; 2012) is a measure within the field of time series analysis that is extensively utilized in literature to assess the volatility spillover across financial markets (e.g. Arouri et al., 2011; Malik and Hammoudeh, 2007; Du et al., 2011; Singh et al., 2019). In general terms, the generalized spillover index is based on a regression model obtained by utilizing time series data and time series regressions.

3.1.1 Time Series Data

A time series dataset consists of a sequence of observations on one, or several, variables over a finite period. The data can be collected at different frequencies, for instance daily, weekly, monthly, quarterly or annually. A key feature that distinguishes time series data from cross-sectional data is temporal ordering, hence precautions must be taken as the past can affect the future. Consequently, observations are often dependent across time, and time series data are therefore difficult to analyze (Wooldridge, 2015). Time series analysis is a technique for drawing inferences concerning time series data. In order to do this, a set of models to represent the data in question is needed (Brockwell et al., 2002). The constructed models have many applications, and they can be categorized as (1) description-, (2) explanation-, (3) prediction- and (4) control models (Chatfield, 2016).

3.1.2 Time Series Regression

There exist several methods for estimating regression models using time series data. Methods include, for instance, ordinary least squares (OLS) and maximum likelihood estimation (MLE) (Walpole et al., 2016). This thesis will focus on the former. OLS is a method for estimating the parameters of a regression model, with the purpose of constructing a model that analyzes the

causal relationship between variables of interest. For illustrational purpose, consider the case of a simple regression model:

$$y_t = \beta_0 + \beta_1 x_t + u_t. \tag{3.1}$$

Equation (3.1) is assumed to hold for the entire population of interest and illustrates a model that explains the dependent variable y_t in terms of the independent variable x_t. The error term u_t, contains all other factors than x_t that affect y_t, and this feature allows capturing the ceteris paribus effect of x_t on y_t. To put it another way, β_1 is the effect of x_t on y_t holding all other factors fixed. However, this does not hold unless an assumption restricting the relationship between x_t and u_t are made.

$$E(u_t|x_t) = E(u_t) \tag{3.2}$$

$$E(u_t) = 0 \tag{3.3}$$

Assumption (3.2) states that the average error term, given the value of x_t, is constant throughout the entire population and (3.3) states that the average error term of the population is zero. By combining assumption (3.2) and (3.3) we get the zero conditional mean assumption, $E(u_t|x_t) = 0$, as well as $Cov(x_t, u_t) = 0$.

$$Cov(x_t, u_t) = E(x_t u_t) = 0 \tag{3.4}$$

If assumption (3.2) holds, β_1 in equation (3.1) is an estimate of the ceteris paribus effect of x_t on y_t.

In order to estimate the intercept and slope parameters of the population regression model (3.1), β_0 and β_1, sample data of the population is required. Equation (3.3) and (3.4) can be rewritten in terms of the dependent variable y_t, the independent variable x_t, and the parameters β_0 and β_1:

$$E(y_t - \beta_0 - \beta_1 x_t) = 0, \tag{3.5}$$

$$E[x_t(y_t - \beta_0 - \beta_1 x_t)] = 0. \tag{3.6}$$

These equations imply two restrictions on the joint probability distribution of x_t and y_t in the population. In order to find the sample counterparts of equations (3.5) and (3.6), estimated parameters of the interception and slope parameters, $\hat{\beta}_0$ and $\hat{\beta}_1$, are introduced.

$$\frac{1}{n}\sum_{t=1}^{n}\left(y_t - \hat{\beta}_0 - \hat{\beta}_1 x_t\right) = 0 \tag{3.7}$$

$$\frac{1}{n}\sum_{t=1}^{n} x_t\left(y_t - \hat{\beta}_0 - \hat{\beta}_1 x_t\right) = 0 \tag{3.8}$$

By applying the basic properties of the summation operator on equation (3.7), the expression can be simplified to:

$$\hat{\beta}_0 = \bar{y} - \hat{\beta}_1 \bar{x}, \tag{3.9}$$

where $\bar{y} = \frac{1}{n}\sum_{t=1}^{n} y_t$ is the sample average of the y_t and similarly for $\bar{x}$. Equation (3.9) is an estimate of the intercept $\hat{\beta}_0$, and can be calculated once the slope $\hat{\beta}_1$ is known. An estimate of $\hat{\beta}_1$ can be found by combining equation (3.8) and (3.9):

$$\hat{\beta}_1 = \frac{\sum_{t=1}^{n}(x_t - \bar{x})(y_{ti} - \bar{y})}{\sum_{t=1}^{n}(x_t - \bar{x})^2} = \frac{Cov(x_t, y_t)}{Var(x_t)}. \tag{3.10}$$

From equation (3.9) and (3.10), $\hat{\beta}_0$ and $\hat{\beta}_1$ are the ordinary least squares (OLS) estimates of β_0 and β_1. Furthermore, the OLS estimates of the parameters are used to construct a sample counterpart of (3.1), which is a fitted linear model for y_t:

$$\hat{y}_t = \hat{\beta}_0 + \hat{\beta}_1 x_t. \tag{3.11}$$

Given an observation x_t in the sample, equation (3.11) gives a fitted value for y_t. The difference between the actual value of y_t and the fitted value $\hat{y}_t$ is commonly referred to as the residual for the observation at time *t*:

$$\hat{u}_t = y_t - \hat{y}_t = y_t - \hat{\beta}_0 + \hat{\beta}_1 x_t. \tag{3.12}$$

One of the important aspects of the OLS estimates, is that the parameters $\hat{\beta}_0$ and $\hat{\beta}_1$ is chosen to minimize the sum of squared residuals (SSR):

$$\sum_{t=1}^{n} \hat{u}_t^2 = \sum_{t=1}^{n}\left(y_t - \hat{\beta}_0 + \hat{\beta}_1 x_t\right)^2. \tag{3.13}$$

By using the $\hat{\beta}_0$ and $\hat{\beta}_1$that minimizes the SSR, the OLS regression line can be defined as:

$$\hat{y}_t = \hat{\beta}_0 + \hat{\beta}_1 x_t, \tag{3.14}$$

which predicts the value of y_t by using the observations x_t in the sample. It is important to remember that these predictions are estimates (Wooldridge, 2015).

According to Wooldridge (2015), the fundamental assumption in the simple regression model stating that all other factors affecting y_t is uncorrelated with x_t is unrealistic. Therefore, drawing ceteris paribus conclusions from simple regression models are often very difficult. If one suspect that several factors simultaneously affect y_t, multiple regression analysis is more suitable as it allows to explicitly control for many factors. The multiple regression model:

$$y_t = \beta_0 + \beta_1 x_{t1} + \beta_2 x_{t2} + \beta_3 x_{t3} + \cdots + \beta_k x_{tk} + u_t \tag{3.15}$$

is an extension of the simple regression model (3.1), where $\beta_1, \dots, \beta_k$ are slope parameters and β_0 is the intercept parameter. The error term u_t, contains all other factors than $x_{t1}, \dots, x_{tk}$ affecting y_t. Similar to simple regression, sample data of the population is needed in order to estimate the parameters of the multiple regression model:

$$\hat{y}_t = \hat{\beta}_0 + \hat{\beta}_1 x_{t1} + \hat{\beta}_2 x_{t2} + \hat{\beta}_3 x_{t3} + \cdots + \hat{\beta}_k x_{tk}. \tag{3.16}$$

The OLS estimates of the parameters $\hat{\beta}_0, \hat{\beta}_1, \dots, \hat{\beta}_k$ are obtained by the same approach as the simple regression case. For multiple regression models the parameters are simultaneously chosen to make the SSR as small as possible:

$$minimize \left[\sum_{t=1}^{n} \left(y_t - \hat{\beta}_0 - \hat{\beta}_1 x_{t1} - \hat{\beta}_2 x_{t2} - \hat{\beta}_3 x_{t3} - \cdots - \hat{\beta}_k x_{tk} \right)^2 \right]. \tag{3.17}$$

Equation (3.17) can be solved by applying linear algebra, which extends the equation to a matrix of $k + 1$ linear equations and $k + 1$ unknow parameters (Wooldridge, 2015).

3.1.3 Assumptions

Several assumptions must be stated in order to justify OLS estimates for time series regression in general terms. The first assumption (TS.1) states that the stochastic process between the dependent variable y_t, and the independent variables x_{ti} is described by the linear model:

$$y_t = \beta_0 + \beta_1 x_{t1} + \beta_2 x_{t2} + \beta_3 x_{t3} + \cdots + \beta_k x_{tk} + u_t, \tag{TS.1}$$

and that the stochastic process is assumed to be stationary and weakly dependent for all time points *t*. Weakly dependence implies that the law of large numbers (LLN) and the central limit theorem (CLT) are applicable. (TS.1) also implies that lags of both dependent and independent variables can be included. Further, it is assumed no perfect collinearity (TS.2). This means that none of the independent variables are constant nor exhibit a perfect linear combination of the

other independent variables. Similar to assumption (3.2), large sample time series analysis assumes that the independent variables x_{ti} are contemporaneously exogenous:

$$E(u_t|x_t) = 0. \tag{TS.3}$$

This means that the independent variables are uncorrelated with the error term of the same time period. However, the independent variables can be correlated with the error term of other periods. Under assumption (TS.1) through (TS.3), the OLS estimators are consistent, meaning:

$$\operatorname{plim}_{n\to\infty} \hat{\beta}_j = \beta_j, j = 0, 1, \dots, k.$$

Moreover, assuming the error terms are contemporaneously homoscedastic[4]:

$$Var(u_t|x_t) = \sigma^2, \tag{TS.4}$$

and that no autocorrelation between the error terms exist:

$$E(u_t u_s|x_t, x_s) = 0, for\ all\ t \neq s, \tag{TS.5}$$

the OLS estimators for the parameters are asymptotically normally distributed. This means that the OLS estimators are approximately normal distributed for large samples. Given assumption (TS.1) through (TS.5), the usual inference procedures are approximately valid for large samples (Wooldridge, 2015).

3.1.4 Stationarity and non-stationarity

When utilizing the generalized spillover index developed in Diebold and Yilmaz (2009; 2012), the input data has to satisfy the criteria of stationarity. In general terms, stationarity means that the probability distribution of the time series process is independent of time. That is to say, the following criteria must be satisfied:

1. Constant expected value, $E(X_t) = \mu$
2. Constant variance, $Var(X_t) = \sigma^2$
3. Covariance of x_t and x_{t+h}, for all t and $h \geq 1$ is independent of time, $Cov(X_t, X_{t+h}) = g(h) \neq f(t)$

A process is said to be covariance stationary if the above criteria are satisfied, and the second moment is finite. In other words, this means that $E(X_t^2) < \infty$ (Bårdsen and Nymoen, 2014). An example of a non-stationary process is a process that exhibit trend. Trend is when a time series

[4] Homoscedasticity is when the variance of the error terms of a regression model is constant, and hence does not vary across time (Wooldridge, 2015).

tends to increase, or decrease, over time and fluctuate around its trend. At a minimum, a trending time series violate the first criterion, $E(X_t) = \mu(t)$, as the mean will be time dependent (Wooldridge, 2015). A trending series can be trend-stationary, and it can be transformed into a stationary series by removing the trend (Enders, 2015).

3.2 Vector Autoregression

The regression model in which the generalized spillover index developed in Diebold and Yilmaz (2009; 2012) is based upon, is a vector autoregression model. Vector autoregression is an extension of an autoregression model, where lags of several variables in the same model can be included. The number of lags to include can be determined by a set of criteria, including the Schwarz criterion, Akaike`s information criterion, Hannan-Quinn criterion and the final prediction error. A vector autoregression can also be represented as a moving average or in companion form. Vector autoregression forms the basis of forecast error variance decomposition, which then is used to obtain the volatility spillovers.

3.2.1 The Autoregression Model

An autoregression model (AR) relates a time series variable to its own lagged values through OLS regression. For illustrational purposes, consider the population's 1st-order autoregressive model, AR(1):

$$Y_t = \beta_0 + \beta_1 Y_{t-1} + u_t. \tag{3.18}$$

Equation (3.18) is a 1st-order autoregressive model because it only includes one lag as independent variable to forecast the dependent variable. In equation (3.18) the intercept and slop parameter, β_0 and β_1, are in practice unknown. To that end, by using historical sample data for the variable of interest OLS estimators of the parameters, $\hat{\beta}_0$ and $\hat{\beta}_1$, can be found:

$$\hat{Y}_{T+1|T} = \hat{\beta}_0 + \hat{\beta}_1 Y_T, \tag{3.19}$$

where the subscript $\hat{Y}_{T+1|T}$ is the forecasted value of Y_{T+1} using information up until time *T*. The difference between $\hat{Y}_{T+1|T}$ and the realization Y_{T+1} is the forecast error:

$$e_{T+1|T} = Y_{T+1} - \hat{Y}_{T+1|T}. \tag{3.20}$$

A common measure of the forecast error is the root mean squared forecast error (RMSFE):

$$RMSFE = \sqrt{E\left(Y_{T+1} - \hat{Y}_{T+1|T}\right)^2}. \tag{3.21}$$

RMSFE measures the magnitude of a typical mistake made by the AR model, which originates from the fact that the error term u_t is a random variable with unknown future values, as well as the estimation errors concerning the parameters β_0 and β_1. The AR(1) model forecasts future values based on just one lagged value. The model simply ignores information from periods further back in time which may contain useful information. Therefore, the general case of a p[th]-order autoregressive model proves useful:

$$Y_t = \beta_0 + \beta_1 Y_{t-1} + \beta_2 Y_{t-2} + \cdots + \beta_p Y_{t-p} + u_t. \tag{3.22}$$

The AR(p) model from equation (3.22) represents Y_t as a function of its p lagged values, $Y_{t-1}, Y_{t-2}, \ldots, Y_{t-p}$, and an intercept (Stock and Watson, 2012).

3.2.2 The Vector Autoregression Model

A vector autoregression model (VAR) is an extension of the univariate AR model in the sense that it is an autoregression to a vector of time series variables. A VAR model is a set of N time series regressions, where the independent variables are the lagged values of all N time series. Similar to AR models, a VAR model is referred to as a VAR(p) model where the number of lags is equal to p (Stock and Watson, 2012). For simplicity, consider the 2-variable VAR(1) model:

$$\begin{aligned} Y_{1,t} &= \beta_{10} + \beta_{11} Y_{1,t-1} + \beta_{12} Y_{2,t-1} + u_{1,t}, \\ Y_{2,t} &= \beta_{20} + \beta_{21} Y_{1,t-1} + \beta_{22} Y_{2,t-1} + u_{2,t}. \end{aligned} \tag{3.23}$$

The equations illustrated in (3.23) consist of two time series variables. In the prior equation, $Y_{1,t}$ is the dependent variable, while $Y_{2,t}$ is the dependent variable of the latter. The independent variables of both equations are lagged values of the two variables. This set of equations can be expressed in matrix form:

$$\boldsymbol{Y_t} = v + \phi_1 \boldsymbol{Y_{t-1}} + u_t, \tag{3.24}$$

where $\boldsymbol{Y_t} = \begin{bmatrix} Y_{1,t} \\ Y_{2,t} \end{bmatrix}, v = \begin{bmatrix} \beta_{10} \\ \beta_{20} \end{bmatrix}, \phi_1 = \begin{bmatrix} \beta_{11} & \beta_{12} \\ \beta_{21} & \beta_{22} \end{bmatrix}, and\ u_t = \begin{bmatrix} u_{1,t} \\ u_{2,t} \end{bmatrix}$. The general case of equation (3.24), N-variable VAR(p) model, are illustrated in equation (3.25):

$$\boldsymbol{Y_t} = v + \sum_{i=1}^{p} \phi_i \boldsymbol{Y_{t-i}} + u_t, \tag{3.25}$$

where $\boldsymbol{Y_t}$ is an $N \times 1$ vector of dependent variables, v is an $N \times 1$ vector of intercept terms, ϕ_i is an $N \times N$ matrix of coefficients and u_t is an $N \times 1$ vector of error terms. The error terms are independently and identically distributed (i.i.d.) with zero expected value and covariance matrix Σ. The coefficients of the VAR model are estimated by using OLS estimates as described in subchapter 3.1.2. Equation (3.25) constructs a VAR model consisting of *N* equations as it includes *N* variables (Lütkepohl, 2005).

3.2.3 VAR model selection

VAR model selection is about finding the best model for the sample data. The estimation error of a VAR model increases when the number of variables increases. Hence, it is advantageous to construct a model with as few variables as reasonably possible, because it decreases the number of coefficients to be estimated. The number of coefficients is a function of number of variables and lags included in the model, $N + N^2p$ (Stock and Watson, 2012). A sequence of tests can be performed to determine the appropriate number of lags to include in a VAR model. Tests include, for instance, Schwarz criterion, Akaike's information criterion, Hannan-Quin criterion, and final prediction error criterion (Lütkepohl, 2005). It is crucial to keep in mind the parsimonious principle when constructing a VAR model. According to the parsimonious principle, one should prefer the model with the least variables if several models are adequate (Davidson and MacKinnon, 2004).

3.2.3.1 Schwarz criterion

The Schwarz criterion (SC), also called Bayesian information criterion (BIC), is a method for determining the appropriate order of a VAR model.

$$BIC(p) = ln\left[det\left(\widehat{\sum}_u\right)\right] + (N + N^2p)\frac{ln(S)}{S}, \tag{3.26}$$

where $\det(\widehat{\sum}_u)$ is the determinant of the covariance matrix constructed by the OLS residuals $\hat{u}_t$, *S* is the sample size, *N* is the number of variables and *p* is the order of the VAR model. The BIC estimator of the appropriate order of the VAR, $\hat{p}$, is the value that minimizes the BIC(*p*). Hence, the BIC(*p*) must be calculated for several orders, e. g. $p = 0, 1, 2, \dots, p_{max}$, and the VAR model with the lowest BIC value is the most appropriate. As the coefficients of the VAR model are estimated by OLS the SSR will never increase when adding another variable to the equation. Hence, the first term of equation (3.26) will decrease, or remain unchanged, with an additional variable. However, the second term of equation (3.26) will increase when additional variables are added to the model (Lütkepohl, 2005).

3.2.3.2 Akaike's information criterion

Akaike's information criterion (AIC) and BIC are based on the same intuition, and the only difference among them is that AIC substitute the term $ln(S)$ with 2.

$$AIC(p) = ln\left[det\left(\widehat{\sum}_u\right)\right] + (N + N^2p)\frac{2}{S} \tag{3.27}$$

In general, a smaller decrease in SSR is needed to justify inclusion of an additional variable compared to the BIC test. Keeping in mind the parsimonious principle, the AIC estimate of *p* is not consistent as it tends to overestimate *p* and include to many variables (Stock and Watson, 2012).

3.2.3.3 Hannan-Quinn criterion

Hannan-Quinn criterion (HQ) is similar in shape, as well as interpretation, as BIC and AIC. The procedure is equal, in terms of calculating the HQ(*p*) value for several *p's* and choosing the VAR model that minimizes HQ(*p*):

$$HQ(p) = ln\left[det\left(\widetilde{\sum}_u\right)\right] + (N + N^2p)\frac{2\ln(ln(S))}{S}. \tag{3.28}$$

Note that $\widetilde{\sum}_u$ is obtained from MLE estimation. For small samples HQ tends to estimate a VAR order smaller than AIC, but greater than BIC (Lütkepohl, 2005).

3.2.3.4 Final prediction error

The final prediction error (FPE) criterion is based on minimizing the mean squared forecast error (MSFE). The FPE test for selection of VAR order utilizes the approximate 1-step-ahead MSFE:

$$\sum_{\hat{y}}(1) = \frac{T + Np + 1}{S}\sum_u. \tag{3.29}$$

To be able to determine the VAR order based on equation (3.29), the covariance matrix $\sum_u$ must be replaced with the OLS estimator $\widehat{\sum}_u$:

$$\widehat{\sum}_u(p) = \frac{S}{S - Np - 1}\widetilde{\sum}_u(p), \tag{3.30}$$

where $\widetilde{\sum}_u(p)$ is the MLE of $\sum_u$ obtained by fitting a VAR(*p*) model. Finally, we arrive at the FPE criterion:

$$FPE(p) = \left[\frac{S + Np + 1}{S - Np - 1}\right]^{N} \det\left(\widetilde{\sum}_u(p)\right). \tag{3.31}$$

Equation (3.31) is used to compute the values of the FPE(p) for several VAR models of order $p = 0, 1, \ldots, p_{max}$. After computing the FPE values for several p values, the order that minimizes the FPE criterion is the estimated p value (Lütkepohl, 2005).

3.2.4 Other VAR Representations

The general N-variable VAR(p) model from equation (3.25) can be represented as a moving average (MA) if the model is stationary (Buigut and Valev, 2005), or the model can be represented in companion form representation (Engler and Nielsen, 2009).

3.2.4.1 Moving average representation

To show how a VAR(p) model can be represented as a MA model, consider the bivariate VAR(1) from equation (3.24):

$$\boldsymbol{Y_t} = v + \phi_1 \boldsymbol{Y_{t-1}} + u_t.$$

This equation follows the pattern $\boldsymbol{Y_t} = \phi_1 \boldsymbol{Y_{t-1}} = \phi_1^2 \boldsymbol{Y_{t-2}} = \cdots = \phi_1^{j+1} \boldsymbol{Y_{t-j-1}}$, and equation (3.24) can be transformed to:

$$\boldsymbol{Y_t} = v\left(I_N + \phi_1 + \cdots + \phi_1^j\right) + \phi_1^{j+1} \boldsymbol{Y_{t-j-1}} + \sum_{i=0}^{j} \phi_1^i u_{t-i}, \tag{3.32}$$

where I_N is an $N \times N$ identity matrix. One of the properties of ϕ_1^j, is that it converges to zero as j increases, which cancels out the second term in equation (3.32) as j goes to infinity. This feature simplifies the first term of equation (3.32) to:

$$v\left(I_N + \phi_1 + \cdots + \phi_1^j\right) \underset{j \to \infty}{\longrightarrow} v(I_N - \phi_1)^{-1}. \tag{3.33}$$

Using this, the VAR(1) process can be expressed as:

$$\boldsymbol{Y_t} = \mu + \sum_{i=0}^{\infty} \phi_1^i u_{t-i}, \tag{3.34}$$

where, $\mu = v(I_N - \phi_1)^{-1}$. This can also be shown for the general case of a N-variable VAR(p) model:

$$\boldsymbol{Y_t} = \mu + \sum_{i=0}^{\infty} \phi^i u_{t-i}, \tag{3.35}$$

where $\phi = \begin{bmatrix} \phi_1 & \phi_2 & \cdots & \phi_{p-1} & \phi_p \\ I_N & 0 & \dots & 0 & 0 \\ 0 & I_N & & 0 & 0 \\ \vdots & & \ddots & \vdots & \vdots \\ 0 & 0 & \dots & I_N & 0 \end{bmatrix}$ is a $Np \times Np$ matrix.

The MA representation can be obtained by multiplying (3.35) by matrix $J := [I_N : 0 : \dots : 0]$, which have dimensions $N \times Np$:

$$y_t = J\boldsymbol{Y_t} = J\mu + \sum_{i=0}^{\infty} J\phi^i J' Ju_{t-i} = \mu + \sum_{i=0}^{\infty} A_i u_{t-i}, \tag{3.36}$$

where A_i follows the recursion $A_i = \phi_1 A_{i-1} + \phi_2 A_{i-2} + \cdots + \phi_p A_{i-p}$, and A_0 is an $N \times N$ identity matrix. $A_i = 0 \; for \; i < 0$. The MA representation of a VAR(p) model is useful to realize the variables' forecast variances (Lütkepohl, 2005).

3.2.4.2 Companion form representation

The companion form representation rewrites a VAR(p) model to a VAR(1), and it can be interpreted as a large scale VAR(1) model. This means that any VAR model with order p, can be rewritten in terms of a VAR(1) model:

$$\boldsymbol{Y_t} = \phi \boldsymbol{Y_{t-1}} + u_t, \tag{3.37}$$

where $\boldsymbol{Y_t} = \begin{bmatrix} y_t \\ y_{t-1} \\ \vdots \\ y_{t-p+1} \end{bmatrix}$, $u_t = \begin{bmatrix} u_t \\ 0 \\ \vdots \end{bmatrix}$ and $\phi = \begin{bmatrix} \phi_1 & \phi_2 & \cdots & \phi_{p-1} & \phi_p \\ I_N & 0 & \dots & 0 & 0 \\ 0 & I_N & & 0 & 0 \\ \vdots & & \ddots & \vdots & \vdots \\ 0 & 0 & \dots & I_N & 0 \end{bmatrix}$. I_N is an $N \times N$ identity matrix, and $u_t \sim (0, \Sigma_u)$ (Canova, 2015). For illustrational purposes, consider the 2-variable VAR(2) model where the VAR will be:

$$\begin{bmatrix} Y_{1,t} \\ Y_{2,t} \end{bmatrix} = \begin{bmatrix} \beta_{11}^1 & \beta_{12}^1 \\ \beta_{21}^1 & \beta_{22}^1 \end{bmatrix} \times \begin{bmatrix} Y_{1,t-1} \\ Y_{2,t-1} \end{bmatrix} + \begin{bmatrix} \beta_{11}^2 & \beta_{12}^2 \\ \beta_{21}^2 & \beta_{22}^2 \end{bmatrix} \times \begin{bmatrix} Y_{1,t-2} \\ Y_{2,t-2} \end{bmatrix} + \begin{bmatrix} u_{1,t} \\ u_{2,t} \end{bmatrix}. \tag{3.38}$$

Note that the intercept coefficients are not included in this example. The companion form representation of the VAR model in equation (3.38) will be:

$$\begin{bmatrix} Y_{1,t} \\ Y_{2,t} \\ Y_{1,t-1} \\ Y_{2,t-1} \end{bmatrix} = \begin{bmatrix} \beta_{11}^1 & \beta_{12}^1 & \beta_{11}^2 & \beta_{12}^2 \\ \beta_{21}^1 & \beta_{22}^1 & \beta_{21}^2 & \beta_{22}^2 \\ 1 & 0 & 0 & 0 \\ 0 & 1 & 0 & 0 \end{bmatrix} \times \begin{bmatrix} Y_{1,t-1} \\ Y_{2,t-1} \\ Y_{1,t-2} \\ Y_{2,t-2} \end{bmatrix} + \begin{bmatrix} u_{1,t} \\ u_{2,t} \\ 0 \\ 0 \end{bmatrix}. \tag{3.39}$$

The companion form representation proves useful when, for instance, calculating moment and in deriving parameter estimates (Gambetti, 2017).

3.2.5 Forecast Error Variance Decomposition

Forecast error variance decomposition (FEVD) is a tool for interpreting VAR models. Lütkepohl (2005) argues that forecasting is one of the main objectives of time series analysis. In terms of VAR models, forecasting future values of $Y_{1,t}, Y_{2,t}, \dots, Y_{N,t}$ is based on all information available at time *T,* Ω_T. This information may for example include both past and present values of the variables in question. Time *T* is commonly referred to as the forecast origin, and the number of periods to forecast into the future is the forecast horizon. *H* denotes the periods ahead to predict, and therefore referred to as an *H*-step predictor. The FEVD gives information about the contribution to the error terms in variable *i* from the *H*-step-ahead forecast of variable *j* (Lütkepohl, 2005). In other words, the FEVD tells us what fraction of the *H*-step-ahead error variance when forecasting Y_i is due to Y_j for all j including $j = i$ (Diebold and Yilmaz, 2009).

3.3 Descriptive Statistical Tests

In order to give a description and justification of the time series data utilized in the current thesis, descriptive statistical tests will be conducted. To give a short description of the distribution of the time series data, a Jarque-Bera (JB) test for normality is presented. To justify the adequacy of the OLS regression in terms of assumption (TS.1), a Portmanteau (PM) test for autocorrelation is presented. Finally, as the generalized spillover index strictly requires stationarity, three tests for stationarity will be presented in the current subchapter; (1) Augmented Dickey-Fuller (ADF), (2) Phillips-Perron (PP) and (3) Dickey-Fuller Generalized Least Squares (DF-GLS).

3.3.1 Normality

Testing for normality is of great importance as the usual inference procedures does not hold unless the error terms are normally distributed (Heij et al., 2004). The JB test for normality jointly compares skewness and excess kurtosis of the sample with skewness and excess kurtosis of a normal distribution. As the properties of a normal distribution includes both excess kurtosis and skewness equal to zero, the null hypothesis of the JB test equals these to parameters to zero:

$$H_0: \gamma_1 = 0 \; and \; \gamma_2 - 3 = 0, \tag{3.40}$$

where $\gamma_1$is the skewness and γ_2 is the kurtosis of the sample (Kennedy, 2003). The JB statistics are based on these two characteristics of the underlying distribution:

$$JB = \frac{S}{6}\left(\gamma_1^2 + \frac{(\gamma_2 - 3)^2}{4}\right) \approx \chi_2^2, \tag{3.41}$$

where *S* is the sample size. The JB statistic is asymptotically chi-squared distributed with 2 degrees of freedom, and the null hypothesis is rejected if test statistics exceed the chi-squared critical value (Heij et al., 2004).

3.3.2 Autocorrelation

Assumption (TS.5) states that there should exist no autocorrelation between the error terms $E(u_t u_s | x_t, x_s) = 0$, for all $t \neq s$. Autocorrelation in a variable can be tested by a PM test. By using an approximately asymptotically χ^2-distributed VAR model, similar to the one in equation (3.25), the PM test compares test statistics with the appropriate χ^2-critical value to either reject or keep the null. For large samples and large number of lags, *h*, the PM test statistic is given by:

$$Q_h \approx \chi^2\big(N^2(h-p)\big). \tag{3.42}$$

The null hypothesis, H_0, of the test states that there is no autocorrelation in the residuals. In other words, the residuals are white noise. If the null is rejected, the alternative hypothesis H_1 will conclude with significant autocorrelation (Lütkepohl, 2005).

3.3.3 Stationarity

To ensure that the time series are independent of time, several tests can be conducted. For the stationarity tests to be valid, the error terms are assumed to be normally distributed white noise (Heij et al., 2004). A time series is said to be stationary if the time series do not have a unit root. A unit root means that the slope parameter is equal to one. The most common way to test for unit roots is to base the hypothesis testing on the first difference of a AR(1) model (3.18):

$$\Delta Y_t = \beta_0 + \rho Y_{t-1} + u_t, \tag{3.43}$$

where $\rho = \beta_1 - 1$ and ΔY_t is the first difference of Y_t. The null and alternative hypothesis are:

$$\begin{aligned} H_0&: \rho = 0, \\ H_1&: \rho < 0. \end{aligned} \tag{3.44}$$

This test is commonly referred to as a Dickey-Fuller test (DF). If the null is true the time series has a unit root, similarly if the null is rejected the time series is stationary. As the independent variable, Y_{t-1}, from (3.43) is a first difference, regular t-statistics are not applicable for the DF test. This is because the CLT is no longer valid when first differences are used in the model.

However, the DF test utilizes an asymptotic distribution of the t-statistics with corresponding critical values. Hence, the regular t-statistics for $\hat{\rho}$ can be used, but in conjunction with the asymptotic critical values. The null of the DF test from (3.44) is rejected in favor of the alternative if $t_{\hat{\rho}} < c$, where c is the asymptotic critical values (Wooldridge, 2015).

3.3.3.1 Augmented Dickey-Fuller Test

The difference between the DF test and the ADF test is that the latter uses lagged differences Δy_{t-h} as independent variables to improve the regression. Including lagged differences further improves the regression as it tries to remove autocorrelation in Δy_t. The procedure is still the same as for the DF test with the same hypothesis test as well as the same critical values and rejection rules (Wooldridge, 2015).

3.3.3.2 Phillips-Perron Test

The PP test for unit roots also originates from the DF test. It is different from the DF test as it uses the Newey-West standard error of ρ to deal with autocorrelation in the residuals. Furthermore, by application of the Newey-West standard error the PP test corrects for both autocorrelation and heteroskedasticity of the error terms (Heij et al., 2004). Hence, the PP test can be viewed as an autocorrelation and heteroskedastic robust DF test (Hudson, 2013).

3.3.3.3 Dickey-Fuller General Least Squares

The DF-GLS is another version of the DF test for unit root. The DF-GLS test transforms the time series by application of a generalized least squares (GLS) regression (Elliott et al., 1996; Stock, 1994). This makes the test more robust than the DF test. This is because the GLS is more efficient relative to OLS when the errors are heteroskedastic or correlated across observations (Stock and Watson, 2012). The null and alternative hypothesis are similar to the DF and ADF test (Stock, 1994; Elliott et al., 1996).

3.4 Volatility

According to Rakkestad (2002) volatility is most commonly referred to as an unobserved parameter measuring the size of the fluctuations of a time series. There exist several methods for estimation of the volatility parameter, however the chosen method must be appropriate for the specific case. The methods are often based on either standard deviation or variance of the variables in question. Volatility is a measure of an asset's associated risk, and therefore a parameter of great importance for, for instance, portfolio management (Shu and Zhang, 2006). Crude oil prices are experiencing high levels of volatility. Hence, there exists a considerable

body of research literature investigating the volatility in crude oil prices (e.g. Pindyck, 1990; Pindyck, 2004b; Narayan and Narayan, 2007; Kang et al., 2009).

3.4.1 Historical Volatility

Historical volatility is traditionally computed as the standard deviation of daily returns within a certain period of time (Shu and Zhang, 2006). In order to create a time series of estimated volatilities, the volatility is calculated for each point as a rolling-window standard deviation of daily returns. The historical data included in the rolling-window will be equally weighted, consequently extreme values will impact the estimated volatilities independent of how far away they occurred. When plotting historical volatilities, a large rolling-window size will yield a smooth curved graph that is less sensitive to fluctuations in the underlying time series. A small window analysis will be more sensitive to fluctuations, and hence be less smooth (Rakkestad, 2002).

3.4.2 Squared log-returns

A common method used to estimate the volatility parameter is to use the squared returns or the squared log-returns (Patton, 2011). The squared log-returns is a model-free and unbiased estimator of the volatility, and hence an easy employable and valid estimator (Andersen et al., 2001; Patton, 2011). This volatility estimator is known to provide sufficient in-sample information of the volatility, but when it comes to forecasting the volatility, the estimator is rather noisy and inefficient (Andersen and Bollerslev, 1998). This may lead to unreliable inference of the true volatility (Andersen et al., 2001).

3.4.3 Intraday Volatility

The intraday volatility is calculated based on intraday data. Garman and Klass (1980) introduces two different volatility estimators that utilizes intraday data to extract information from the underlying time series. The first volatility estimator utilizes the maximum and minimum price for the relevant day, while the other estimator utilizes the opening and closing price. Moreover, a combination of the two previously mentioned estimators, using the max, min, open and close price has been used to compute a more efficient estimator of the price volatility (Diebold and Yilmaz, 2009).

3.4.4 Volatility Spillover

Chang et al. (2018) define volatility spillover as the effect of shocks in one variable to the subsequent shock in volatility in another variable. Diebold and Yilmaz (2009) construct a measurement of volatility spillover based on VAR models, primarily the FEVD of the VAR

models. The measure is called the spillover index. For illustrational purposes consider the bivariate VAR(1) model $(Y_{1,t}, Y_{2,t})$, with corresponding error vector:

$$e_{T+1|T} = \boldsymbol{Y_{T+1}} - \widehat{\boldsymbol{Y}}_{\boldsymbol{T+1|T}} = \alpha_0 u_{T+1} = \begin{bmatrix} a_{0,11} & a_{0,12} \\ a_{0,21} & a_{0,22} \end{bmatrix} \begin{bmatrix} u_{1,T+1} \\ u_{2,T+1} \end{bmatrix}, \tag{3.45}$$

and the covariance matrix of the error vector is:

$$E\left(e_{T+1|T}, e'_{T+1|T}\right) = \alpha_0 \alpha'_0. \tag{3.46}$$

From equation (3.45), the variance of the 1-step-ahead error in forecasting $Y_{1,t}$ is $a_{0,11}^2 + a_{0,12}^2$, and similarly for $Y_{2,t}$, $a_{0,21}^2 + a_{0,22}^2$. In the case of a bivariate VAR(1) model there exist two possible spillovers, shock in $Y_{1,t}$ affecting $Y_{2,t}$, and vice versa. In α_0, these spillovers are $a_{0,21}^2$ and $a_{0,12}^2$, respectively. Hence, the total spillover in this case will be the sum of these two, $a_{0,12}^2 + a_{0,21}^2$. The total spillover index is expressed as a ratio, where the total spillover is divided by the total forecast error variance:

$$S = \frac{a_{0,12}^2 + a_{0,21}^2}{a_{0,11}^2 + a_{0,12}^2 + a_{0,21}^2 + a_{0,22}^2} \times 100 = \frac{a_{0,12}^2 + a_{0,21}^2}{trace(\alpha_0 \alpha'_0)} \times 100. \tag{3.47}$$

Remember that (3.47) is for a bivariate VAR(1) model, and the general case of a *N*-variable VAR(*p*) is:

$$S = \frac{\sum_{h=0}^{H-1} \sum_{\substack{i,j=1 \\ i \neq j}}^{N} a_{h,ij}^2}{\sum_{h=0}^{H-1} trace(\alpha_0 \alpha'_0)} \times 100. \tag{3.48}$$

In equation (3.48) the numerator is the sum of the off-diagonal elements, while the denominator is the sum of all elements. The FEVD utilized in Diebold and Yilmaz (2009) are based on Cholesky factorization, which essentially means that the variance decompositions depends on the ordering of the variables (Diebold and Yilmaz, 2012).

4 Data and Methodology

This chapter describes both the oil price data and methodology in which the analysis of this thesis is based upon. More specifically, this chapter includes a classification, as well as descriptive statistics for daily prices, returns and volatilities of all crude oils included in the analysis of the current thesis. Furthermore, this chapter describes the generalized spillover index developed in Diebold and Yilmaz (2009; 2012), as well as a description of how to perform the analysis in the programming software R.

4.1 Data

The data considered in this thesis are daily spot prices for a set of 17 crude oils from May 1996 until January 2019, providing a total of 5480 observations per price series. The considered daily spot prices are closing prices, which is the final price a crude has been traded for at each trading day. The dataset is extracted from Thomson Reuters Eikon, and includes the three major benchmarks (Brent, Dubai and WTI) as well as 14 other regional crudes covering African (Bonny and Forcados), European (Urals), North Sea (Ekofisk and Oseberg), Asian (Tapis, Minas, Duri and North West Australian), Middle Eastern (Murban and Oman) and American (Louisiana Light Sweet, West Texas Sour and Alaskan) crude oils. For simplicity, North West Australian, Louisiana Light Sweet and West Texas Sour will be abbreviated to NWA, LLS and WTS, respectively, for the remainder of this thesis. When price data is missing for one or more price series due to a holiday, price data for all crudes are excluded for this day.

Table 3 provides a summary of the field location and crude oil quality in terms of API gravity, sulfur content and TAN of the crude oil considered in the current thesis. These characteristics are described in subchapter 2.4, and it is further mentioned in the same subchapter that a high-quality crude oil is characterized by a high API gravity, low sulfur content as well as low TAN. As an example, it appears from Table 3 that the NWA crude is of higher quality than the Duri crude. The crudes are sorted by its closest benchmark in terms of field location.

Table 3: Field location, API gravity, sulfur content and total acid number for benchmark and regional crudes.

	Field location	API gravity	Sulfur content	Total acid number
Brent	UK	37.5°	0.40%	0.03
Ekofisk	Norway	38.9°	0.21%	0.10
Oseberg	Norway	39.6°	0.20%	0.12
Urals	Russia	31.8°	1.24%	0.05
Bonny	Nigeria	35.1°	0.15%	0.25
Forcados	Nigeria	31.5°	0.22%	0.33
Dubai	UAE	31.4°	1.96%	0.25
Murban	UAE	40.5°	0.74%	0.05
Tapis	Malaysia	42.7°	0.04%	0.22
Minas	Indonesia	34.5°	0.08%	0.40
Duri	Indonesia	21.1°	0.20%	1.00
Oman	Oman	31.3°	1.41%	0.64
North West Australian	Australia	63.0°	0.00%	0.02
WTI	US	40.6°	0.22%	0.10
Louisiana Light Sweet	US	38.5°	0.40%	0.25
West Texas Sour	US	34.7°	0.81%	0.11
Alaskan	US	32.0°	0.96%	0.17

Table 4 provides an overview of the descriptive statistics for all the price series. It can be observed from the descriptive statistics that the crude oil market is relatively homogenous, where both the price ranges and measures of central tendency are close to equal for all price series. Moreover, the standard deviation is also close to equal for all the price series indicating a similar distribution around the mean of the price series. The correlation between regional markets and their closest benchmark in terms of field location are for all price series close to perfect. These observations in conjunction with Figure 1 of historical benchmark prices indicate an efficient market (Ross et al., 2018). This is in line with other researchers findings that the global crude oil market is highly integrated (Bachmeier and Griffin, 2006).

Table 4: Descriptive statistics of price data. Regional crude oils per closest benchmark in terms of geographical location, and correlation is estimated between regional and closest benchmark.

	Min	Mean	Median	Max	Std.dev	Correlation
Brent	9.14	56.91	52.09	145.36	33.14	1
Ekofisk	9.19	57.39	52.32	146.30	33.65	0.9996
Oseberg	9.35	57.68	52.70	147.43	33.71	0.9996
Urals	8.48	55.20	50.16	139.88	33.03	0.9989
Bonny	9.10	58.01	52.86	148.60	33.99	0.9996
Forcados	9.13	58.09	52.92	148.60	34.36	0.9996
Dubai	9.36	54.53	50.41	140.80	32.34	1
Murban	10.10	57.11	53.02	146.54	33.29	0.9990
Tapis	10.53	60.15	55.34	152.38	35.03	0.9971
Minas	9.55	58.20	55.11	152.83	34.64	0.9951
Duri	8.55	54.52	51.17	135.03	33.10	0.9891
Oman	9.28	55.09	50.89	139.89	32.57	0.9994
North West Australian	10.53	56.98	51.97	140.16	32.72	0.9888
WTI	10.82	55.00	50.59	145.31	29.28	1
Louisiana Light Sweet	10.64	58.30	53.13	149.42	32.84	0.9910
West Texas Sour	9.31	52.10	48.63	142.64	28.44	0.9959
Alaskan	8.72	56.47	51.14	144.72	33.04	0.9888

Table 5 reviews the descriptive statistics for the daily log-returns of the price series[5]. Keep in mind that the log-returns are measured in percentages. As seen from Table 5, the daily returns from the crude oil markets are typically ranging between +/-20%. On the other hand, both the mean and median log-return for all the crude oils are close to zero. The relatively high standard deviations indicate that the log-returns are experiencing high levels of volatility. As noted from Table 4, the price series are close to perfectly correlated, however, the log-returns series experience a lower correlation. These correlations provide the first comparison between the regional crudes and their closest benchmark. Notably, the Asian crudes (Tapis, Minas, Duri and NWA) seem to experience the lowest correlation to their closest benchmark (around 0.5), and Brent with its corresponding regional crudes experience relatively high correlation (around 0.7). The extreme correlation between WTI and the American crude oils may be partially due to the export ban lasting from 1975 to 2015. The export ban created an artificial price differential between the American crudes, in particular depressing the sweet crude relative to the sour crude

[5] Daily log-returns are calculated by taking the natural logarithm of the price at time t divided by the price at t-1: $R = \ln\left(\frac{P_t}{P_{t-1}}\right)$.

(Putnam and Brusstar, 2015). A JB test does reject the null for kurtosis and skewness significantly different for that of a normal distribution for all the price series.

Table 5: Descriptive statistics of daily log-returns (%). Regional crude oils per closest benchmark in terms of geographical location, and correlation is estimated between regional and closest benchmark

	Min	Mean	Median	Max	Std.dev	Corr.	Kurtosis	Skewness
Brent	-18.72	0.02	0.05	16.26	2.41	1	6.677	-0.172
Ekofisk	-20.11	0.02	0.05	18.01	2.35	0.722	7.835	-0.109
Oseberg	-30.49	0.02	0.05	26.94	2.38	0.702	14.723	-0.202
Urals	-20.62	0.02	0.07	18.63	2.48	0.713	7.961	-0.159
Bonny	-19.75	0.02	0.05	17.29	2.28	0.726	7.680	-0.087
Forcados	-19.83	0.02	0.05	16.98	2.29	0.729	7.689	-0.061
Dubai	-18.03	0.02	0.04	19.04	2.37	1	7.557	-0.036
Murban	-16.29	0.02	0.03	14.29	2.28	0.709	7.146	-0.232
Tapis	-14.07	0.02	0.00	14.14	2.11	0.624	6.802	-0.145
Minas	-39.47	0.02	0.00	38.02	2.40	0.508	35.835	-0.554
Duri	-35.36	0.02	0.00	34.09	2.71	0.499	27.166	-0.032
Oman	-19.53	0.02	0.04	15.05	2.43	0.704	7.880	-0.246
North West Australian	-34.13	0.02	0.00	78.49	2.86	0.457	127.930	3.571
WTI	-21.59	0.02	0.08	19.14	2.50	1	8.621	-0.168
Louisiana Light Sweet	-18.94	0.02	0.08	13.77	2.44	0.921	6.633	-0.203
West Texas Sour	-15.91	0.01	0.05	17.70	2.78	0.901	6.120	-0.046
Alaskan	-21.39	0.02	0.08	20.86	2.63	0.911	9.987	-0.197

Note that the NWA crude oil has extreme log-returns, these extreme observations occurred between a period ranging from June 2008 to January 2009. During this period, a major gas production facility on the Varanus Islands (NWA) experienced a series of explosions followed by fires causing close to a third of Western Australia's gas supply to be lost (Hurley et al., 2008). This gas crisis may have led to the extreme price movements during this period for the NWA crude oil.

Table 6 provides a summary of the daily volatilities of all the price series. Due to lack of intraday data, the volatility series are calculated by application of the squared log-returns method. Note that the measures are in percentages. From Table 6 it is evident that the volatilities for the crude oil prices are typically ranging from 0 to 4%. Due to the mathematical properties of the squared log-returns method, negative values will never occur. The extreme volatilities for the NWA crude might be due to the Varanus Islands gas explosions in late 2008. Most crude oil prices considered seem to experience an average volatility close to 0.06 and a standard deviation close to 0.15. Finally, compared to the price series and the daily log-returns, the correlation between the volatility of regional crudes and their closest benchmark are smaller. In

particular, the Dubai benchmark and the Asian regional crudes volatilities experience a low correlation of about 0.1.

Table 6: Descriptive statistics of daily volatility (%). Regional crude oils per closest benchmark in terms of geographical location, and correlation is estimated between regional and closest benchmark.

	Min	Mean	Median	Max	Std.dev	Corr.	Kurtosis	Skewness
Brent	0.000	0.058	0.000	3.506	0.139	1	136.974	8.848
Ekofisk	0.000	0.055	0.000	4.045	0.144	0.661	229.606	11.820
Oseberg	0.000	0.057	0.000	9.294	0.210	0.432	979.971	26.323
Urals	0.000	0.061	0.000	4.250	0.162	0.627	230.236	12.038
Bonny	0.000	0.052	0.000	3.901	0.135	0.670	246.423	12.212
Forcados	0.000	0.052	0.000	3.932	0.136	0.677	239.913	12.030
Dubai	0.000	0.056	0.000	3.623	0.143	1	179.727	10.346
Murban	0.000	0.052	0.000	2.653	0.129	0.711	100.617	8.094
Tapis	0.000	0.045	0.000	2.000	0.107	0.514	91.730	7.627
Minas	0.000	0.058	0.000	15.582	0.339	0.129	1424.301	33.859
Duri	0.000	0.073	0.000	12.506	0.375	0.180	566.236	21.087
Oman	0.000	0.059	0.000	3.813	0.155	0.669	133.882	9.193
North West Australian	0.000	0.082	0.000	61.611	0.921	0.090	3661.849	56.252
WTI	0.000	0.063	0.000	4.661	0.173	1	187.824	10.781
Louisiana Light Sweet	0.000	0.059	0.000	3.586	0.141	0.784	135.971	8.766
West Texas Sour	0.000	0.077	0.000	3.134	0.175	0.771	65.388	6.508
Alaskan	0.000	0.069	0.000	4.577	0.207	0.828	182.624	11.223

Table 7 provides a summary of the descriptive statistical tests for the volatility series. These tests are explained in subchapter 3.3. The JB test rejects the null of normality for all the volatility series, and the PM test rejects the null of zero autocorrelation. All the stationarity tests, ADF, PP and DF-GLS, conclude that the volatility series are stationary. Note that all tests are statistically significant at 0.01% level. To summarize, the tests performed on the volatility series conclude that they experience non-normal distribution, autocorrelation and stationarity.

Table 7: Descriptive statistical tests for the daily volatilities of the price series. All tests are statistically significant at 0.01% level.

	JB	PM	ADF	PP	DF-GLS
Brent	-	144.43	-42.74	-62.73	-42.45
Ekofisk	-	61.17	-45.92	-66.53	-39.58
Oseberg	-	10.23	-37.25	-70.85	-34.51
Urals	-	35.29	-46.67	-68.27	-40.13
Bonny	-	46.90	-46.53	-67.43	-39.89
Forcados	-	45.91	-46.54	-67.49	-39.90
Dubai	-	347.11	-41.89	-57.08	-38.16
Murban	-	261.45	-42.43	-59.15	-41.89
Tapis	-	147.13	-43.04	-62.64	-41.55
Minas	-	824.44	-41.26	-49.18	-41.15
Duri	-	639.02	-42.59	-51.86	-42.59
Oman	-	231.10	-38.97	-59.87	-38.63
North West Australian	-	68.53	-48.35	-66.13	-48.33
WTI	-	186.38	-41.93	-61.29	-41.81
Louisiana Light Sweet	-	219.70	-40.30	-60.23	-33.35
West Texas Sour	-	192.35	-41.99	-61.10	-41.92
Alaskan	-	235.51	-43.15	-59.87	-41.61

4.2 Methodology

To evaluate the volatility spillover between crude oil markets, the present study utilizes the generalized version of the spillover index developed in Diebold and Yilmaz (2009; 2012). The generalized spillover index developed in these papers can be calculated in the programming software R.

4.2.1 Generalized Spillover Index

Whilst the spillover index developed in Diebold and Yilmaz (2009) explained in subchapter 3.4.4 is order dependent and solely focus on total spillover, the generalized version utilized in this thesis allows for identification of directional spillovers, net spillovers and net pairwise spillovers in a non-order dependent framework. This is because the method utilizes the generalized VAR framework developed in Koop et al. (1996) and Pesaran and Shin (1998) rather than Cholesky factorization to obtain the FEVD (Diebold and Yilmaz, 2012). This framework will hereafter be referred to as KPPS (Koop, Potter, Pesaran and Shin). The generalized spillover index can identify the volatility spillover across time and between several markets, as well as the spillover direction from one market to another (Kang et al., 2017). The methodology allows identification of both main receivers and transmitters of volatility across several markets (Dahl and Jonsson, 2018). The generalized spillover index can be used to perform both *full-sample* and *rolling-window* analysis. A full-sample analysis captures the

average connectedness over the sample data, whilst a rolling-window analysis captures the time-varying connectedness (Diebold and Yilmaz, 2012).

4.2.2 Deriving the Generalized Spillover Index

In order to derive the generalized spillover index, consider the general case of a covariance stationary *N*-variable VAR(*p*) model as described in chapter 3:

$$\boldsymbol{Y_t} = v + \sum_{i=1}^{p} \phi_i \boldsymbol{Y_{t-i}} + u_t, \tag{4.1}$$

where $\boldsymbol{Y_t}$ is an $N \times 1$ vector of dependent variables, v is an $N \times 1$ vector of intercept terms, ϕ_i are $N \times N$ matrices of autoregressive coefficients and u_t is an $N \times 1$ vector of error terms. The error terms are assumed to be i.i.d. with expectation zero and covariance matrix Σ, $u \sim (0, \Sigma)$. In order to obtain the FEVD for equation (4.1), a transformation into MA representation is required:

$$\boldsymbol{Y_t} = \mu + \sum_{i=0}^{\infty} \boldsymbol{A_i} u_{t-i}. \tag{4.2}$$

Importantly, the moving average coefficients from equation (4.2) are the fundamental key to understand the dynamics of the system in question (Diebold and Yilmaz, 2012). Given market shocks to the system, it is possible to identify the FEVD from each variable via the MA coefficients (Dahl and Jonsson, 2018). That is to say, the FEVD enables the possibility of measuring the fraction of the *H*-step-ahead error variance from forecasting y_i that is due to market shocks to y_j for all $j = 1, 2, \ldots, N$ (Diebold and Yilmaz, 2012).

4.2.2.1 Forecast error variance decomposition

In order to understand the practical intuition of FEVD, it is important to understand the concept of own-variance shares and cross-variance shares. Diebold and Yilmaz (2012) define own-variance shares as the fraction of the *H*-step-ahead error variance from forecasting y_i that is due to market shocks to y_i for all *N* variables. Further, the authors define cross-variance shares as the fraction of the *H*-step-ahead error variance from forecasting y_i that is due to market shocks to y_j for all $j \neq i$. Cross-variance shares are also referred to as spillovers. Equation (4.3) yields the *H*-step-ahead FEVD based on the KPPS framework where θ_{ij}^{g} denotes the fraction of the *H*-step-ahead forecast error variance from forecasting y_i that is due to market shocks to y_j. This equation is applicable for calculation of both own-variance shares and cross-variance shares:

$$\theta_{ij}^{g}(H) = \frac{\sigma_{jj}^{-1} \sum_{h=0}^{H-1} \left(e_i' A_h \sum e_j\right)^2}{\sum_{h=0}^{H-1} (e_i' A_h \sum A_h' e_i)}, \tag{4.3}$$

where $\sum$ is the covariance matrix for the error term vector u_t. The standard deviation of the error term for the *j*-th equation is given by σ_{jj}, and e_i is a selection vector with all elements equal to zero, except the *i*-th element, which is set to one. The resulting FEVD from equation (4.3) can be tabulated as in Table 8 for $i, j = 1, 2, \ldots, N$.

Table 8: Illustration of a FEVD table.

	From			
To	**1**	**2**	**...**	**N**
1	θ_{11}^{g}	θ_{12}^{g}	...	θ_{1N}^{g}
2	θ_{21}^{g}	θ_{22}^{g}	...	θ_{2N}^{g}
⋮	⋮	⋮	⋱	⋮
N	θ_{N1}^{g}	θ_{N2}^{g}	...	θ_{NN}^{g}

According to Diebold and Yilmaz (2012; 2015) the row sum of Table 8 is not always equal to one, this can be solved by normalizing each element, θ_{ij}^{g}, by dividing by the row sum in the following way:

$$\tilde{\theta}_{ij}^{g}(H) = \frac{\theta_{ij}^{g}(H)}{\sum_{j=1}^{N} \theta_{ij}^{g}(H)}. \tag{4.4}$$

The normalized version of Table 8 is obtained by substituting each element with the output from equation (4.4), and this forces the row sums to unity (Diebold and Yilmaz, 2012).

4.2.2.2 Generalized total spillover index

The generalized total spillover index is obtained by dividing the sum of the off-diagonal elements of the normalized FEVD table by the sum of all table elements. The off-diagonal elements are the cross-variance shares, or spillovers.

$$S^{g}(H) = \frac{\sum_{\substack{i,j=1 \\ i \neq j}}^{N} \tilde{\theta}_{ij}^{g}(H)}{\sum_{i,j=1}^{N} \tilde{\theta}_{ij}^{g}(H)} \times 100 \tag{4.5}$$

Equation (4.5) represents the KPPS total spillover index analogous to the total spillover index derived in subchapter 3.4.4. In general terms, the total spillover index is the relative contribution of spillovers compared to the total forecast error variance (Diebold and Yilmaz, 2012).

4.2.2.3 Generalized directional spillovers and net spillovers

One of the main advantageous of the generalized spillover method developed in Diebold and Yilmaz (2009; 2012) relative to other methods for calculating spillover is that it enables the possibility of directional spillovers between markets to be identified (Kang et al., 2017). The directional spillover received by market *i* from all other markets *j* is obtained by dividing the row sum of cross-variance shares for market *i* by the sum of all FEVD normalized elements:

$$S_{i.}^{g}(H) = \frac{\sum_{j=1}^{N} \tilde{\theta}_{ij}^{g}(H)}{\sum_{i,j=1}^{N} \tilde{\theta}_{ij}^{g}(H)} \times 100. \quad (4.6)$$

Equation (4.6) yields the volatility spillover received by market *i*. Similarly, the volatility transmitted from market *i* to all markets *j* can be calculated with the following equation:

$$S_{.i}^{g}(H) = \frac{\sum_{j=1}^{N} \tilde{\theta}_{ji}^{g}(H)}{\sum_{i,j=1}^{N} \tilde{\theta}_{ij}^{g}(H)} \times 100. \quad (4.7)$$

The numerator of equation (4.7) is the column sum of the cross-variance shares for market *i*, and the denominator is again the sum of all FEVD normalized elements (Diebold and Yilmaz, 2012). The net volatility spillover from market *i* to all market *j* is the difference between the volatility transmitted and received by market *i*:

$$S_{i}^{g}(H) = S_{.i}^{g}(H) - S_{i.}^{g}(H). \quad (4.8)$$

4.2.2.4 Generalized net pairwise spillovers

While equation (4.8) yields information about net volatility spillover from market *i* to all markets *j*, the net pairwise volatility spillovers are the difference between the gross volatility transmitted from market *i* to another market *j* as well as those transmitted from market *j* to market *i* (Diebold and Yilmaz, 2012). According to the authors, the net pairwise volatility spillovers can be defined as in equation (4.9):

$$S_{ij}^{g}(H) = \left(\frac{\tilde{\theta}_{ji}^{g}(H)}{\sum_{i,k=1}^{N} \tilde{\theta}_{ik}^{g}(H)} - \frac{\tilde{\theta}_{ij}^{g}(H)}{\sum_{j,k=1}^{N} \tilde{\theta}_{jk}^{g}(H)} \right) \times 100. \quad (4.9)$$

4.2.3 The Generalized Spillover Index in R

In the current thesis, R is utilized to obtain the generalized spillover index. R is a programming language and -software that facilitates data manipulation, calculation and graphical displays. It is possible to extend R by installing packages developed by R and via the CRAN, which is the

Comprehensive R Archive Network (R-Project, 2019). In order to compute the generalized spillover index, it is necessary to install the package "frequencyConnectedness" from CRAN. In general, the methodology in R can be divided into three parts; (1) construction of a VAR model, (2) computing the FEVD table and (3) calculate the various spillovers.

4.2.3.1 Construction of a VAR model

The following function can be applied to construct a VAR(p) model in R:

VAR(y, p = 1, type = c("const", "trend", "both", "none")),

where y is the dependent variables to include in the VAR(p) model, and p is the number of lags included. The number of lags included is by default set to $p = 1$. The *type* argument determines which deterministic regressors to include, and the options are to include a constant, trend, both or none of them. As described in the theoretical background chapter, the number of lags to include in the VAR(p) model can be determined by minimizing a set of information criteria (SC, AIC, HQ and FPE). This process can be conducted in R with the following function:

VARselect(y, lag.max = 10, type = c("const", "trend", "both", "none")).

It is the same arguments in the *VARselect* function as in the *VAR* function described above, and the additional *lag.max* argument specifies the maximum number of lags to test for. This argument is by default set to 10. The output from this function suggests how many lags to include according to all four information criteria (Pfaff and Stigler, 2018).

4.2.3.2 Computing the forecast error variance decomposition table

In order to create and store the normalized FEVD table for further spillover analysis, the following function is required:

spilloverDY12(est, n.ahead = H, no.corr = F/T).

In the case of computing spillovers, the *est* argument refers to the VAR(p) model constructed by the *VAR* function described above. How many steps ahead the FEVD should be predicted for is determined by the *n.ahead* argument. As an example, if *n.ahead* = H the H-step-ahead FEVD will be computed. In general, H should be set high enough so that the elements of the FEVD table do not change with a unit increase in H. The *no.corr* argument determines whether the off-diagonal elements of the covariance matrix, Σ, should be set to zero (*T*) or not (*F*) (Krehlik, 2018). The *spilloverDY12* function computes the normalized FEVD table based on the entire dataset defined in the *VAR* function, and this is the basis for a full-sample analysis (Diebold and Yilmaz, 2009; Krehlik, 2018). A full-sample analysis yields a single fixed-parameter for the

volatility spillovers by capturing the average spillover behavior over the entire sample period (Diebold and Yilmaz, 2009).

A rolling-window analysis can be conducted to capture potentially time-varying spillover behavior instead of just the average spillover behavior over the sampled data (Diebold and Yilmaz, 2012). This is beneficial because the volatility of commodity prices are known to be varying across time (Pindyck, 2001). The rolling-sample analog to the *spilloverDY12* function described above is:

spilloverRollingDY12(y, n.ahead = H, no.corr, func_est, params_est, window).

The arguments *y*, *n.ahead* and *no.corr* are the same as previously described. The *func_est* argument defines which model to estimate, and it can be set to either VAR or BigVAR. The *params_est* defines which parameters to include in the estimation of the model. The *window* argument defines the length of the rolling-window (Krehlik, 2018), and the size of the window will determine the resolution of the analysis. A larger window will result in a smoother curve, whilst a smaller window will increase the resolution of the resulting graphs (Diebold and Yilmaz, 2009).

4.2.3.3 Full-sample analysis and rolling-window analysis

In a full-sample analysis, it is possible to capture the total, directional, net, and net pairwise volatility spillovers on an average basis (Diebold and Yilmaz, 2012). After generating the FEVD table by using either the *spilloverDY12* function for full-sample analysis, or *spilloverRollingDY12* for rolling-window analysis, the total volatility spillover can be calculated using the function:

overall(spillover_table).

For directional, net, and net pairwise volatility spillover the following functions can be applied, respectively:

to(spillover_table),
from(spillover_table),
net(spillover_table), and
pairwise(spillover_table).

The *spillover_table* argument refers to the FEVD table generated by the functions mentioned above. For directional spillovers, the *to* function computes the spillover transmitted from market *i* to all markets *j*. The *from* function computes the spillover received by market *i* from all market

j. The *net* function subtracts the received from the transmitted volatility spillover to give the net volatility spillover as output. The net pairwise volatility spillover between market *i* and market *j* is computed by using the *pairwise* function (Krehlik, 2018). These functions generate a single fixed-parameter in a full-sample analysis, and for a rolling-window analysis they generate a time series revealing time varying information about the volatility spillovers.

5 Empirical results

In this chapter, we utilize the generalized spillover index developed in Diebold and Yilmaz (2009; 2012) to explore volatility spillover within the crude oil market. For this purpose, we perform both full-sample and rolling-window analyses of volatility spillovers between (1) crude oil benchmarks (Brent, Dubai and WTI), (2) Brent and regionals (Ekofisk, Oseberg, Urals, Bonny and Forcados), (3) Dubai and regionals (Murban, Tapis, Minas, Duri, Oman and NWA), and (4) WTI and regionals (LLS, WTS and Alaskan). Both the full-sample and rolling-window analyses are conducted in the programming software R as described in chapter 4. Furthermore, we will interpret the results in light of typical determinants affecting crude oil prices over time, such as global oil supply and demand, inventories, OPEC decisions, financial crises, national elections and geopolitical unrest.

When utilizing the generalized spillover index to perform both full-sample and rolling-window analysis of the volatility spillovers within the crude oil market, a covariance stationary *N*-variable VAR(p) model as described in equation (3.25) is required. The variables included in the abovementioned analyses (1, 2, 3 and 4) are a set of daily volatilities for each crude oil, hence the number of variables in each analysis is equal to the number of crudes included. For instance, the analysis of the benchmark crudes includes three variables corresponding to the daily volatilities of Brent, Dubai and WTI. As previously mentioned, the variables included in the analysis must satisfy the criteria of stationarity. As observed in Table 7, the daily volatility series for all 17 crude oils are stationary according to the ADF, PP and DF-GLS tests.

In order to determine the number of lags to include in the VAR(p) model for each analysis (1, 2, 3 and 4), a sequence of tests is performed. These tests are described in subchapter 3.2.3, and include minimizing the information criteria SC, AIC, HQ and FPE. In the current thesis, p_{max} has been set to 10 lags, and the results of the tests are presented in Table 9. For illustrational purposes, values for only lags of 1 and 10 are included in the table. According to the information criteria from Table 9, in conjunction with the parsimonious principle, the number of lags included in the VAR(p) model for all analyses is set to 1. This is because of the marginal difference in the information criteria values for lags of 1 and 10.

Table 9: VAR model selection; SC, AIC, HQ and FPE for all analyses.

Analysis	**(1)**		**(2)**		**(3)**		**(4)**	
Lags	1	10	1	10	1	10	1	10
SC	-39.6	-39.7	-89.5	-89.7	-89.7	-90.3	-54.4	-54.4
AIC	-39.7	-39.8	-89.6	-90.2	-89.8	-90.9	-54.4	-54.6
HQ	-39.7	-39.7	-89.6	-90.0	-89.7	-90.7	-54.4	-54.4
FPE	0.0	0.0	0.0	0.0	0.0	0.0	0.0	0.0

As mentioned in the methodology chapter, the *H*-step predictor should be set high enough so that the elements of the FEVD table do not change with a unit increase in *H*. The FEVD table remained unchanged in all four cases approximately at $H = 10$, which is equivalent to two business weeks. To summarize, the analyzes of volatility spillovers within crude oil markets are based on covariance stationary 3-, 6-, 7-, and 4-variable VAR(1) model for each analysis, respectively, and the *H*-step predictor is set to 10 for all analyses.

5.1 Analysis of Crude Oil Benchmarks

This part includes the empirical results from both the full-sample and rolling-window analysis of volatility spillover between the benchmark crudes Brent, Dubai and WTI. These specific benchmarks are chosen as they cover the vast majority of global crudes, where Brent covers Europe and Africa, Dubai covers the Middle East and WTI covers America.

5.1.1 Full-Sample Analysis of Volatility Spillover

In this part, a full-sample analysis of the volatility spillover between benchmark crudes is conducted, and the results are tabulated in Table 10. This table is often referred to as a volatility spillover table. A volatility spillover table is simply a summary of all the spillovers (total, directional and net) in addition to the normalized FEVD table explained in the methodology subchapter. Keep in mind that the elements on the diagonal of the FEVD table are the own-variance shares, and the off-diagonal elements are the spillovers (or cross-variance shares). The table elements are presented as percentages, and as the FEVD table elements are normalized according to equation (4.4), the row sum is forced to equal 100%. Note that the "directional to others" and "directional from others" elements are the volatility spillover transmitted and received by each market *i*, respectively.

Table 10: Volatility spillover table for all benchmarks (Brent, Dubai and WTI). Note: diagonal elements show own-variance shares, and off-diagonal elements show cross-variance shares. Directional FROM and TO others are estimated by equation (4.6) and (4.7), respectively. Total spillover index and net spillover are estimated by equation (4.5) and (4.8), respectively.

	Brent	**Dubai**	**WTI**	**Directional FROM others**
Brent	68.34	11.22	20.43	31.65
Dubai	5.06	91.64	3.30	8.36
WTI	21.48	8.10	70.42	29.58
Directional TO others	26.55	19.32	23.73	**Total spillover index:**
Directional including own	94.89	110.96	94.15	23.20%
Net spillover	-5.11	10.96	-5.85	

It is evident from the full-sample analysis that the volatility spillover between the benchmarks accounts for 23.20% of the volatility in the respective markets, indicating a moderate connectedness between the benchmark crudes. The own-variance shares explain most of the volatility for all three benchmarks, indicating that most of the volatility in each individual market comes from within the market itself. In particular, the own-variance share for Dubai is very high, suggesting that it does not receive much volatility from the two other benchmarks. For directional volatility spillovers, the average behavior between the benchmarks is that Brent and WTI are net receivers, while Dubai is a net transmitter of volatility. As seen in Table 10, almost one-third of the volatility in the Brent and WTI benchmarks are received from the two other markets.

To further emphasize the direction of the spillover, Table 11 presents the net pairwise spillover between the benchmarks, and the results reveal that Brent is a net receiver from Dubai, and a net transmitter to WTI. Further, WTI is a net receiver from both markets, whilst Dubai is a net transmitter to both Brent and WTI. These findings suggest that, on average, Dubai is the most significant contributor to uncertainty in the global crude oil market.

Table 11: Net pairwise spillover table for all benchmarks (Brent, Dubai and WTI). The net pairwise spillovers are estimated by equation (4.9).

Net pairwise spillover			
	Brent	**Dubai**	**WTI**
Brent	0	6.16	-1.05
Dubai	-6.16	0	-4.80
WTI	1.05	4.80	0

Remember that the full-sample analysis only captures the average behavior of volatility spillover over the sample data, and to capture the time-varying dynamics of the volatility spillover, a rolling-window analysis is conducted. However, the full-sample analysis provides a great starting point for further analysis of the volatility spillover behavior.

5.1.2 Rolling-Window Analysis of Volatility Spillover

In this part, a rolling-window analysis of the volatility spillover is conducted, and both windows of 100 and 250 days are utilized. Note that 250 days are the equivalent of a business year. The analysis starts off by assessing the total volatility spillover index as calculated by equation (4.5), and the results are plotted in Figure 4. The upper panel illustrates the total volatility spillover index for a rolling-window of 100 days, while the lower panel is for a rolling-window of 250 days. At first glance, the two plots are very similar. However, a key distinction is that the plot for a rolling-window of 250 days tends to smooth out fluctuations. Because the resolution of the plot for a rolling-window of 100 days is higher, the analysis will mainly focus on the upper panel.

Both the volatility spillover index in the upper and lower panel are typically ranging between 10 and 40%, with an average volatility of about 25%. This is consistent with the findings from the full-sample analysis. Furthermore, it is apparent from Figure 4 that the total volatility spillover index does not exhibit any clear trend over the sample period, and that the volatility spillover is indeed time-varying. These findings are in line with Pindyck (2001).

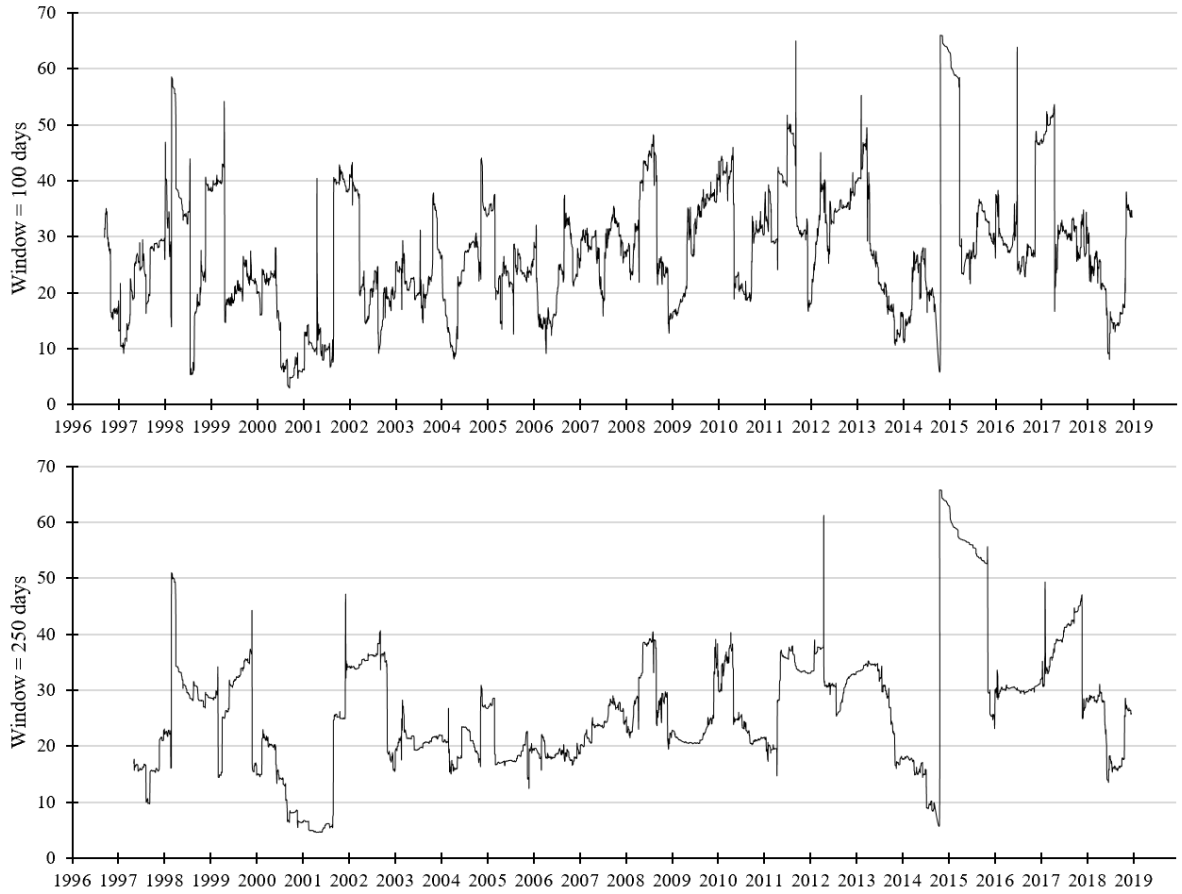

Figure 4: Total volatility spillover index for crude oil benchmarks.

As previously mentioned, the vast majority of the spillovers are ranging between 10 and 40%. However, several peaks above 50% are identified over the sample (March 1998, May 1999, September 2011, February 2013, November 2014, July 2016 and December 2016).

The first two peaks in connectedness may have been related to the East Asian Crisis. As described in subchapter 2.1, the East Asian crisis was associated with a 50% drop in oil price. In a period preceding 1997, emerging economies in East Asia experienced a substantial economic growth accompanied with industrialization and increasing oil consumption. However, in 1997-98 the financial system of East Asian countries experienced severe stress, causing doubt in the market about future growth in these countries. Nevertheless, the East Asian crisis appeared to be short-termed, and the volatility spillover spike in May 1999 may have been related to the resumed growth in the emerging economies of East Asia (Hamilton, 2011). Furthermore, the increase in connectedness during these periods may have be further exacerbated by OPEC-meetings. Firstly, a study by Plante (2019) reveals that the oil price experienced increased volatility associated with an OPEC-meeting in March 1998 where they decided to cut production despite agreeing to increase production at the November 1997-meeting. Secondly, OPEC decided to further decrease production in an early 1999-meeting as

an attempt to increase the oil price (Barsky and Kilian, 2004; Fattouh, 2007). These OPEC decisions, in conjunction with the East Asian crisis may have caused the two first peaks in connectedness.

As mentioned and described in subchapter 2.7.1, the period from 2003 until 2008 was characterized by a relatively steep increase in oil price due to, for instance, rising demand of crude oil from emerging economies in East Asia. According to Kilian and Hicks (2013), the economic growth during this period was not solely for emerging economies, but also the case for industrialized economies. The total volatility spillover index for the benchmark crudes is also stable during this period of increasing oil prices and strong economic growth globally. This observation is apparent from both panels in Figure 4.

The rapid increase in connectedness starting in December 2010 and climaxing with a spike in September 2011 and February 2013 may be associated with the unrest caused by the Arab Spring. Notably, political unrest and wars in the Middle East may cause severe changes in the oil price due to shifts in supply (Barsky and Kilian, 2004). As mentioned in subchapter 2.1, geopolitical unrest such as the Arab Spring may cause uncertainty about future scarcity of oil, and hence an increase in oil price volatility. The Arab Spring started with a rebellion in Tunisia late 2010, causing a domino effect across North-Africa and the Middle East resulting in, among others, regime changes in Tunisia, Egypt, and Libya as well as civil wars in Yemen and Syria (Leraand, 2017). During the Arab Spring, several oil fields and refineries were attacked in Libya (Bahgat, 2012), and Yemen and Syria struggled to maintain their current production levels (Stevens, 2012). Such events may have caused increased uncertainty about future supply of oil, and therefore increased connectedness between the benchmark crudes.

As mentioned in subchapter 2.7.1, disturbances on the supply and demand side have caused large fluctuations in the oil price throughout history. Therefore, the high connectedness between the benchmark crudes in December 2010, September 2011 and February 2013 may have been further exacerbated by the U.S. shale oil revolution which caused an excess supply of light sweet crudes in the U.S. market due to lack of appropriate infrastructure to manage the increased production (Kilian, 2016). Figure 5 illustrates estimates of U.S. oil production per region. Note the rapid increase starting in 2011. The U.S. refineries did not have the required equipment to deal with the increased supply of light sweet crude, and the lack of refinery demand caused oil abundance in Cushing, Oklahoma. Further, this caused a price fall of WTI relative to Brent (Kilian, 2016), which may have caused excess spillover in the global crude oil market. On the other hand, Baumeister and Kilian (2016b) provide evidence that the Brent benchmark

underperformed by $10 from 2011 to mid-2014 due to the U.S. fracking boom. Significantly, the authors further state that the fracking boom had severe consequences for Saudi Arabia's financial reserves, both in terms of lost oil revenues and reduction of their foreign exchange reserves. Thus, the spikes in December 2010, September 2011 and February 2013 may have been related to both geopolitical unrest during the Arab Spring and the U.S. fracking boom.

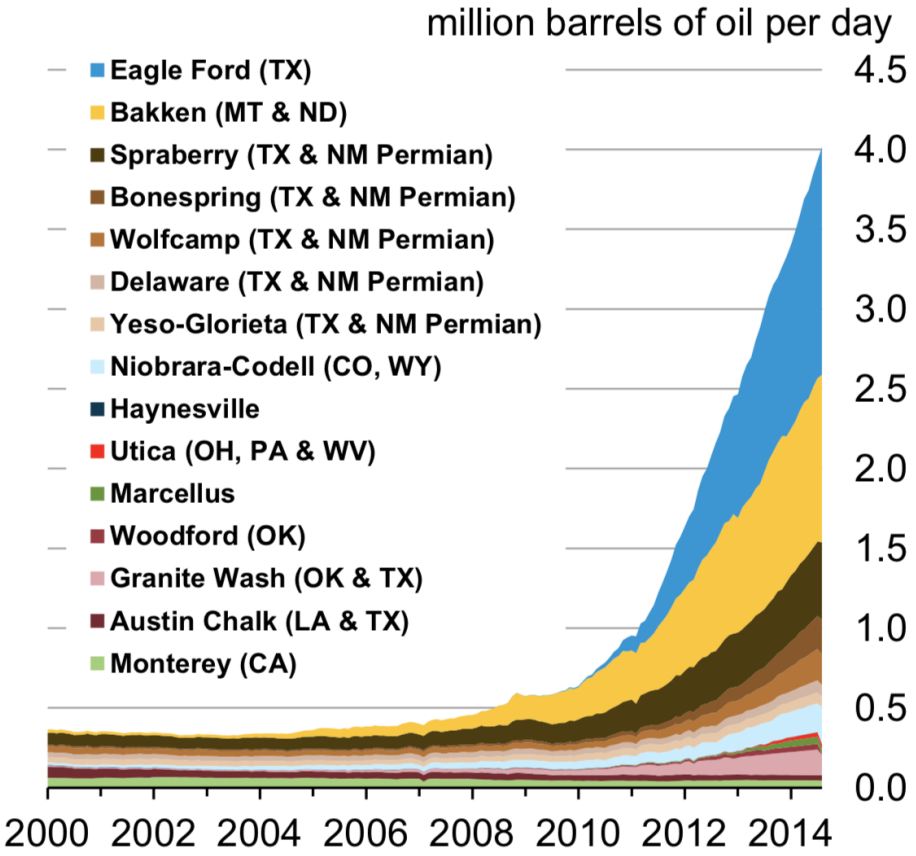

Figure 5: EIA estimates of U.S. oil production per region (Sieminski, 2014).

In November 2014 the connectedness jumps from 7 to 66%, making it the biggest jump over the sampled data. As explained in subchapter 2.2, OPEC decisions to maintain current production level have a significant effect on oil price volatility. Hence, the spike in connectedness may be related to the fact that OPEC announced to maintain their current production levels, despite the increasing production levels in non-OPEC countries. Importantly, Russia and the U.S. both contributed by increasing their daily production in the second half of 2014 by 2 and 4%, respectively. During the same period, the total increase in production from non-OPEC countries was close to 400,000 barrels per day (Baumeister and Kilian, 2016b). Despite the increasing oil production in Russia, they suffered several sanctions on their petroleum sector from the European Union and the U.S. due to their military interventions in Crimea, Ukraine (Fjaertoft and Overland, 2015). These sanctions in conjunction with Russian

troops entering Ukraine in November and the OPEC decision to maintain production might have had an impact on the jump in connectedness in November 2014 (BBC, 2014).

The last two peaks in connectedness may be related to the 2016 U.S. presidential election, where Donald Trump represented the Republicans and Hillary Clinton the Democrats. As the world-leading oil producer, the U.S. presidential election may have caused turbulence in the global crude oil market because of the candidates' opposing views on unconventional oil extraction via hydraulic fracturing. Whilst Donald Trump favored further development of the U.S. shale production, Hillary Clinton wanted to put strict regulations on hydraulic fracturing (Evensen, 2016). According to the American election polls from RealClearPolitics (2016) preceding the 2016 U.S. presidential election, Hillary Clinton was leading the entire time except for a short period in July which coincides with the July 2016 peak of benchmark connectedness. Despite the polls indicating in favor of Democratic victory, Donald Trump won the election. The 2016 election shock may have caused the December 2016 spike, which coincides with the announcement of the election results.

Thus far, the rolling-window analysis has only focused on the total volatility spillover, and hence no information about the directional spillover has been provided. Figure 6 presents information about how the directional spillover between each benchmark varies over time. Each line represents the net pairwise spillover between two benchmarks. A positive value indicates that the first mentioned benchmark in the legend is a net receiver, while a negative value indicate that the second benchmark is a net receiver.

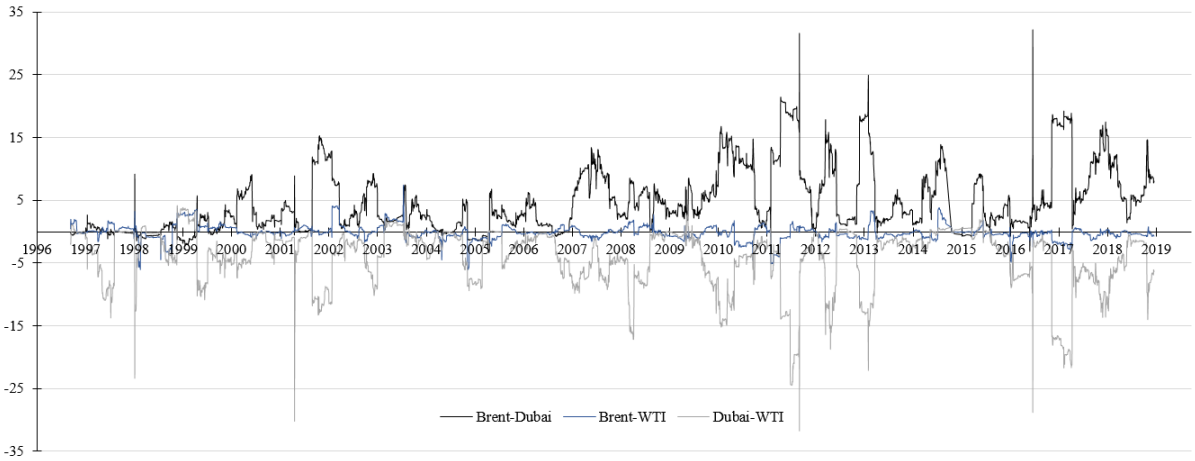

Figure 6: Net pairwise volatility spillovers between benchmark crudes.

The results presented in Figure 6 are in line with the findings from the full-sample analysis. In particular, it provides compelling evidence that Brent and WTI are net receivers from Dubai across the entire sample. This finding may signify the importance of paying attention to the

Middle East when assessing the uncertainty in the global crude oil market. For instance, a study by Bhar et al. (2008) concludes that Dubai is the most sensitive benchmark in terms of major geopolitical events in Iran, Nigeria, Venezuela and the Middle East. Henceforth, this strengthens the findings that the geopolitical unrest during the Arab Spring increased the connectedness between the global benchmarks from December 2010 to February 2013. This can also be observed from Figure 6, where the net volatility spillover from Dubai to WTI and Dubai to Brent is between 15 and 25% during the same period.

While the net spillover between Dubai and the other two benchmarks appears to be one-directional across the entire sample, the net spillover between Brent and WTI ranges between +/-5% and is frequently changing direction. The fact that it is fluctuating around zero indicates that both markets transmit equal amount of volatility to each other.

In order to further investigate the importance of the Dubai benchmark in terms of volatility in the global crude oil market, it is interesting to analyze the amount transmitted from each benchmark to the others over the entire sample period. The volatility transmitted from each benchmark crude is illustrated in Figure 7.

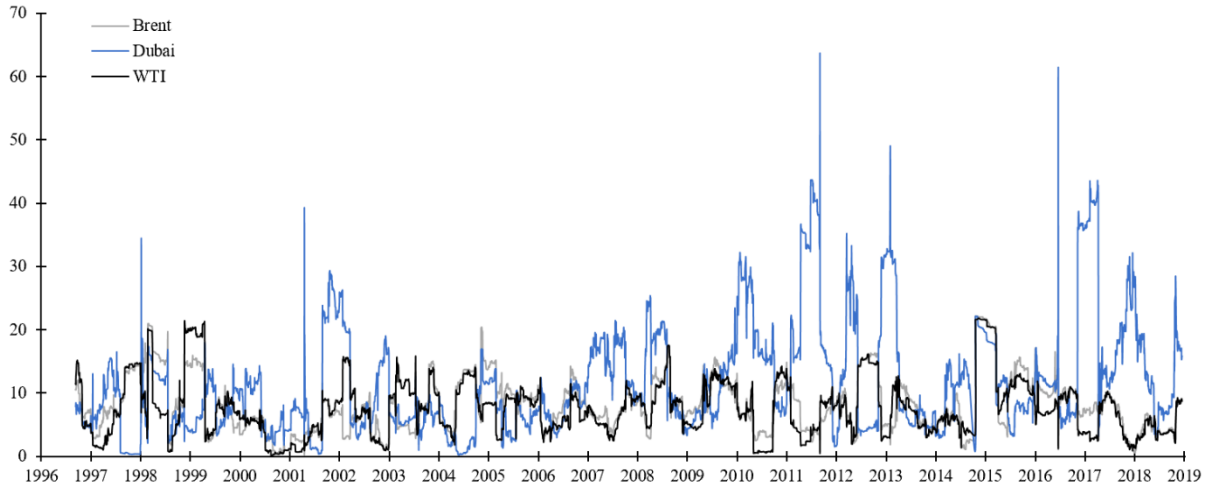

Figure 7: Volatility spillover from benchmark crudes TO others.

As seen from Figure 7, the Dubai benchmark is generally transmitting more than both Brent and WTI throughout the entire period. Dubai often exceeds the other benchmarks by more than 25 percentage points, but the Dubai crude also has minor periods where it transmits far less volatility than the other crudes.

It is interesting to note the behavior of volatility transmitted from Dubai before and after the initiation of the Arab Spring in 2011. Dubai and the other benchmarks are transmitting similar amount of volatility before the Arab Spring, whilst after the initiation Dubai is transmitting far

more volatility than the other two benchmarks. This observation in conjunction with the findings in Bhar et al. (2008) suggests that Dubai not only is the most sensitive benchmark to geopolitical unrest, but it also transmits the increased volatility to the other global markets.

5.2 Analysis of Brent and Regionals

This part includes the empirical results from both the full-sample and rolling-window analysis of volatility spillover between Brent and regionals. The crudes included in this analysis are the benchmark Brent, and the regional crudes Ekofisk, Oseberg, Urals, Bonny and Forcados. Both Ekofisk and Oseberg are Norwegian crudes (North Sea), Urals is a Russian crude, and Bonny and Forcados are both Nigerian crudes. The European crudes are included in this analysis due to their geographic vicinity to Brent, while Bonny and Forcados are included due to their chemical similarities to Brent.

5.2.1 Full-Sample Analysis of Volatility Spillover

The results from the full-sample analysis of volatility spillover between Brent and regionals are presented in Table 12. As mentioned previously, a volatility spillover table includes total, directional and net spillover for all variables included in the VAR(p) model.

Table 12: Volatility spillover table for Brent and regionals. Note: diagonal elements show own-variance shares, and off-diagonal elements show cross-variance shares. Directional FROM and TO others are estimated by equation (4.6) and (4.7), respectively. Total spillover index and net spillover are estimated by equation (4.5) and (4.8), respectively.

	Brent	**Ekofisk**	**Oseberg**	**Urals**	**Bonny**	**Forcados**	**Directional FROM others**
Brent	33.18	15.19	6.31	13.96	15.53	15.83	66.82
Ekofisk	9.68	21.35	8.77	19.28	20.49	20.42	78.64
Oseberg	6.82	14.74	35.38	13.83	14.64	14.59	64.62
Urals	9.02	19.90	8.49	21.98	20.29	20.32	78.02
Bonny	9.80	20.27	8.62	19.46	21.03	20.81	78.96
Forcados	9.95	20.17	8.57	19.47	20.80	21.03	78.96
Directional TO others	45.27	90.27	40.76	86.00	91.75	91.97	**Total spillover index:**
Directional including own	78.45	111.62	76.14	107.98	112.78	113.00	74.30 %
Net Spillover	-21.55	11.63	-23.86	7.98	12.79	13.01	

The total spillover index in the lower right corner of Table 12 suggests a high connectedness on average between Brent and its corresponding regional crudes. The average behavior over the sample is that a total of 74.30% of the volatility in all six crudes originate from spillover effects. Similar to the analysis of the benchmark crudes, the own-variance shares are the main contributor to the volatility in each crude. Despite the geographical location of Bonny and

Forcados (Nigeria) compared to the others (Europe), it is interesting to note the amount transmitted from these crudes to the others (around 92%). On the other hand, this may be due to their chemical similarities in terms of API gravity, sulfur content and TAN compared to the European crudes. From the spillover table, it is evident that Brent and Oseberg are net receivers, whilst Ekofisk, Urals, Bonny and Forcados are net transmitters of volatility.

Table 13 presents the net pairwise volatility spillover for Brent and the regional crudes.

Table 13: Net pairwise spillover table for Brent and regionals. The net pairwise spillovers are estimated by equation (4.9).

Net pairwise spillover						
	Brent	**Ekofisk**	**Oseberg**	**Urals**	**Bonny**	**Forcados**
Brent	0	5.51	-0.51	4.94	5.73	5.88
Ekofisk	-5.51	0	-5.97	-0.62	0.22	0.25
Oseberg	0.51	5.97	0	5.34	6.02	6.02
Urals	-4.94	0.62	-5.34	0	0.83	0.85
Bonny	-5.73	-0.22	-6.02	-0.83	0	0.01
Forcados	-5.88	-0.25	-6.02	-0.85	-0.01	0

On average, it appears that all regional crudes except Oseberg are net transmitters of volatility to their geographically closest benchmark, Brent. This finding suggests that the Brent benchmark behaves as a volatility buffer for the regional crudes. This implies that the Brent benchmark reduces the uncertainty in the regional crudes by receiving volatility. Moreover, from Table 12 it can be seen that the regional crudes account for a total of 66.82% to the volatility in Brent on average over the entire sample.

5.2.2 Rolling-Window Analysis of Volatility Spillover

The rolling-window analysis of volatility spillover between Brent and regionals starts by assessing the total volatility spillover index illustrated in Figure 8. In general, the crudes are experiencing high connectedness across the entire sample, typically ranging between 70 and 80%. It is apparent from both the upper and lower panel (window of 100 and 250 days, respectively) that the connectedness is relatively stable within this range. However, both panels indicate a drop from 82 to 66% in March 1998. This drop may be related to the East Asian crisis. Figure 6 provides compelling evidence for this hypothesis as it can be seen from this figure that the Dubai benchmark accounts for about 10% of the volatility in Brent in March 1998. Meaning that the connectedness between Brent and its regionals reduces because they receive volatility from the Asian market due to the East Asian crisis.

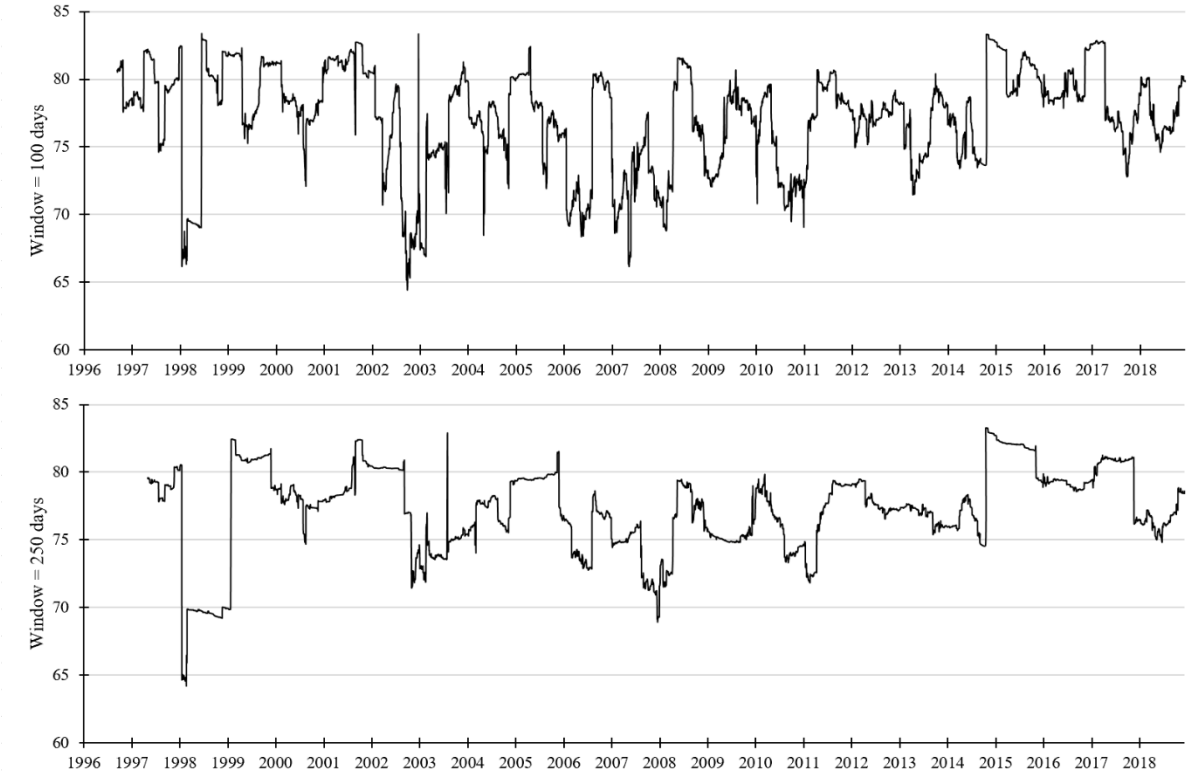

Figure 8: Total volatility spillover index for Brent and regionals.

As suggested in the full-sample analysis, the Brent benchmark appears to behave as a volatility buffer for the regional crudes on average over the sample. To further investigate this hypothesis, it is interesting to analyze the net pairwise spillover between Brent and its regionals across time. The results from this analysis are illustrated in Figure 9. A positive value indicate that Brent is a net receiver of volatility, whilst a negative value indicates the opposite.

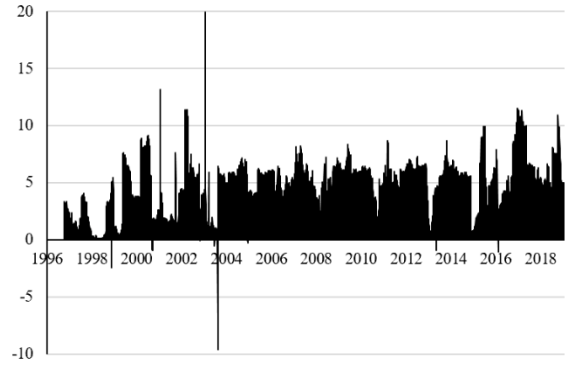

Panel A: From Ekofisk to Brent

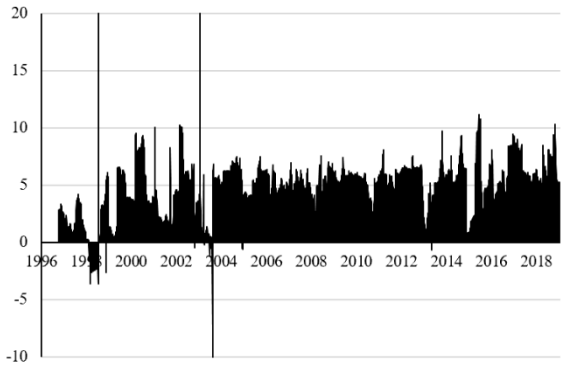

Panel B: From Oseberg to Brent

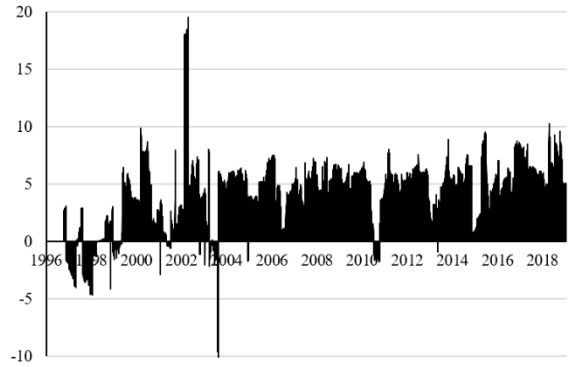

Panel C: From Urals to Brent

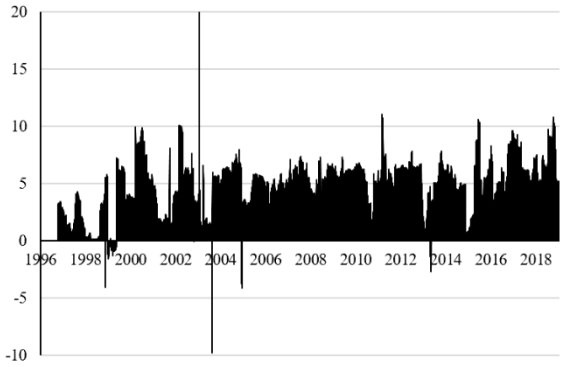

Panel D: From Bonny to Brent

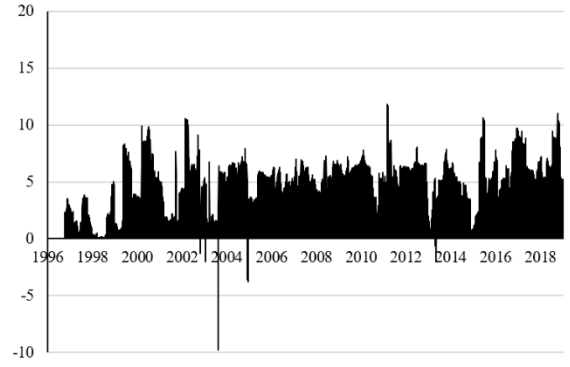

Panel E: From Forcados to Brent

Figure 9: Net pairwise volatility spillovers between Brent and regionals.

As seen from Figure 9, only with a few rare exceptions, Brent is a net receiver of volatility from all the regional crudes over the entire sample. The net volatility spillover received by Brent is relatively stable between 5 and 10% from all the regional crudes over the entire sample period. These observations further strengthen the hypothesis of Brent behaving as a volatility buffer for the regional crudes. Interestingly, Brent does not only behave as a volatility buffer for the crudes in the immediate vicinity, but also for the crudes further away from the North Sea. This may be due to their similarities in chemical and physical properties to the Brent benchmark (ref. Table 3).

5.3 Analysis of Dubai and Regionals

This part includes the empirical results from both the full-sample and rolling-window analysis of volatility spillover between Dubai and regionals. The crudes included in this analysis are the benchmark Dubai, and the regional crudes Murban, Tapis, Minas, Duri, Oman and NWA. These crudes are chosen as they cover the Middle East (Dubai, Murban and Oman), and the Asian-Pacific market (Tapis, Minas and Duri) as well as Australia (NWA). Remember from subchapter 2.5 that Dubai is used as a benchmark for crude oils flowing east from the Middle East.

5.3.1 Full-Sample Analysis of Volatility Spillover

The results of the full-sample analysis (including total, directional and net spillovers) of the Dubai crude and its regional crudes are presented in Table 14. Over the full sample period, the total spillover index implies a relatively high connectedness between Dubai and its regional crudes. The total spillover index reveals that, on average, less than half of the volatility in the seven crudes is due to spillover effects (48.81%). Once again, the own-variance shares are the main contributor of volatility in each crude. In particular, the NWA crude has a very high own-variance share (81.21%) compared to the other six crudes in this sample, indicating a low connectedness between NWA and the other crudes of this analysis. This may be because of its geographical location, the fact that it is of a different quality than the other crudes, or a combination.

Table 14: Volatility spillover table for Dubai and regionals. Note: diagonal elements show own-variance shares, and off-diagonal elements show cross-variance shares. Directional FROM and TO others are estimated by equation (4.6) and (4.7), respectively. Total spillover index and net spillover are estimated by equation (4.5) and (4.8), respectively.

	Dubai	**Murban**	**Tapis**	**Minas**	**Duri**	**Oman**	**NWA**	**Directional FROM others**
Dubai	43.81	22.51	11.36	0.70	1.44	20.07	0.11	56.19
Murban	18.04	35.49	13.30	0.72	1.28	30.85	0.32	64.51
Tapis	12.14	17.86	46.56	2.59	3.52	16.76	0.56	53.43
Minas	1.27	0.97	2.88	59.46	34.23	1.15	0.04	40.54
Duri	1.78	1.86	3.78	33.45	55.62	2.91	0.59	44.37
Oman	16.19	31.74	12.80	0.78	1.96	36.19	0.35	63.82
NWA	1.21	3.00	6.36	0.67	4.62	2.93	81.21	18.79
Directional TO others	50.63	77.94	50.48	38.91	47.05	74.67	1.97	**Total spillover index:**
Directional including own	94.44	113.43	97.04	98.37	102.67	110.86	83.18	48.81 %
Net spillover	-5.56	13.43	-2.95	-1.63	2.68	10.85	-16.82	

The results show that most of the crudes are transmitting about 50% volatility to the other crudes in this sample. Interestingly, the NWA crude is very different compared to the other crudes of

this analysis, and this may once again be due to its geographical location. However, if the volatility moving between Minas and Duri is excluded, both crudes are very close to NWA in terms of volatility transmitted. This may follow the same argument as for NWA, because both Minas and Duri are Indonesian crudes, and the highest contribution to volatility transmitted from the two crudes are between themselves. Interestingly, this is not the case for the Malaysian crude Tapis. Tapis appears to transmit more volatility to Dubai relative to the other Asian crudes, and this may be due to its chemical similarities to the Middle Eastern crudes.

The regional crudes account for a total of 56.19% of the volatility in their geographically closest benchmark, Dubai, on average. The amount received from the regional crudes seems to be highly dependent on the geographic proximity relative to Dubai. In particular, the Middle Eastern crudes Murban and Oman transmit about 20% each to Dubai, whilst the Malaysian crude Tapis transmits 11.36% and the Indonesian and Australian crudes transmit about 1% each to Dubai.

The net pairwise spillover table presented in Table 15 reveals that Dubai is on average a net receiver of volatility from both the Middle Eastern crudes Murban and Oman, while it is a net transmitter to Tapis, Minas, Duri and NWA. This once again signifies the importance of geographical location in this analysis.

Table 15: Net pairwise spillover table for Dubai and regionals. The net pairwise spillovers are estimated by equation (4.9).

Net pairwise spillover							
	Dubai	**Murban**	**Tapis**	**Minas**	**Duri**	**Oman**	**NWA**
Dubai	0	4.47	-0.78	-0.57	-0.34	3.88	-1.10
Murban	-4.47	0	-4.56	-0.25	-0.58	-0.89	-2.68
Tapis	0.78	4.56	0	-0.29	-0.26	3.96	-5.80
Minas	0.57	0.25	0.29	0	0.78	0.37	-0.63
Duri	0.34	0.58	0.26	-0.78	0	0.95	-4.03
Oman	-3.88	0.89	-3.96	-0.37	-0.95	0	-2.58
NWA	1.10	2.68	5.80	0.63	4.03	2.58	0

5.3.2 Rolling-Window Analysis of Volatility Spillover

In order to analyze the time-varying spillover effects between Dubai and its regional crudes, a rolling-window analysis is conducted. The results from the rolling-window analysis of the total volatility spillover index are plotted in Figure 10 (for both windows of 100 and 250 days). At first glance, it seems that the total volatility spillover index for Dubai and its regional crudes experiences immense fluctuations around the mean of approximately 65%. The total spillover ranges from a minimum of 24% to a maximum of 86% over the sample period. These extreme

values provide points of interest in terms of market connectedness, and they occur in September 1997 and November 2014, respectively. These two points of interest are the most prominent points from both panels in Figure 10. As indicated in the benchmark analysis, Dubai plays a vital role in the global crude oil market in terms of volatility spillover. With this in mind, the low connectedness observed in September 1997 between Dubai and regionals can also be found in the total volatility spillover plot from the benchmark analysis (ref. Figure 4). This illustrates the influence Dubai has on the volatility in the global crude oil market. This hypothesis is further strengthened by the low amount transmitted from Dubai to the other benchmarks from Figure 7. The September 1997 drop in connectedness may be related to the East Asian crisis.

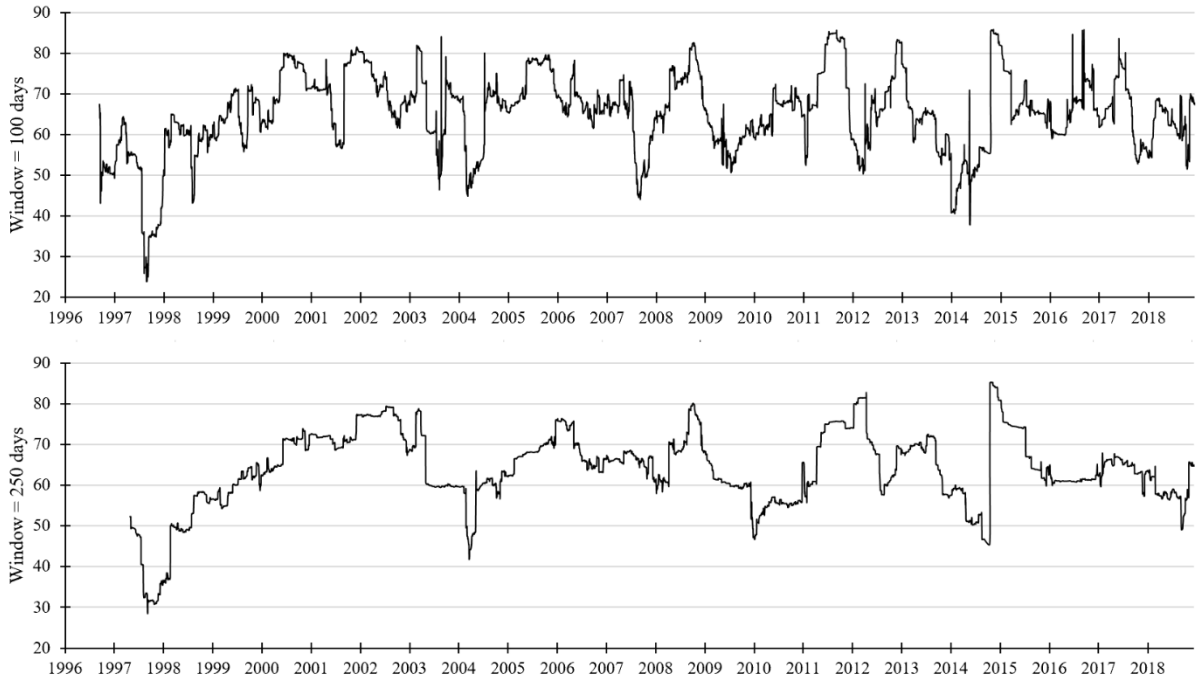

Figure 10: Total volatility spillover index for Dubai and regionals.

Similar to the observation in September 1997, the connectedness in November 2014 from both Figure 4 and Figure 10 experience a joint movement, except this time it is spiking. Again, in terms of volatility, this illustrates the influence Dubai has on the global oil market. The supply-shock mentioned in the benchmark analysis might be the explanation of the rapid increase in connectedness between Dubai and its regionals in November 2014.

To further investigate the relationship between Dubai and its regional crudes it is interesting to analyze the net pairwise spillover for Dubai against the other crudes. Figure 11 is plotted to illustrate the aggregated net volatility spillovers between Dubai and the regional crudes. In general, up until 2013 the Dubai benchmark was switching between being a net receiver and net transmitter of volatility for all regional crudes considered in this analysis. After 2013, a

regime shift occurred in terms of spillover effects. From 2013 until 2019, Dubai was a net receiver of about 14% throughout the entire period from all the regional crudes aggregated. This period is characterized by unrest related to the Arab Spring, and the observations from Figure 11 may suggest that the Dubai benchmark behaved as a volatility buffer throughout this period of geopolitical unrest in the Middle East.

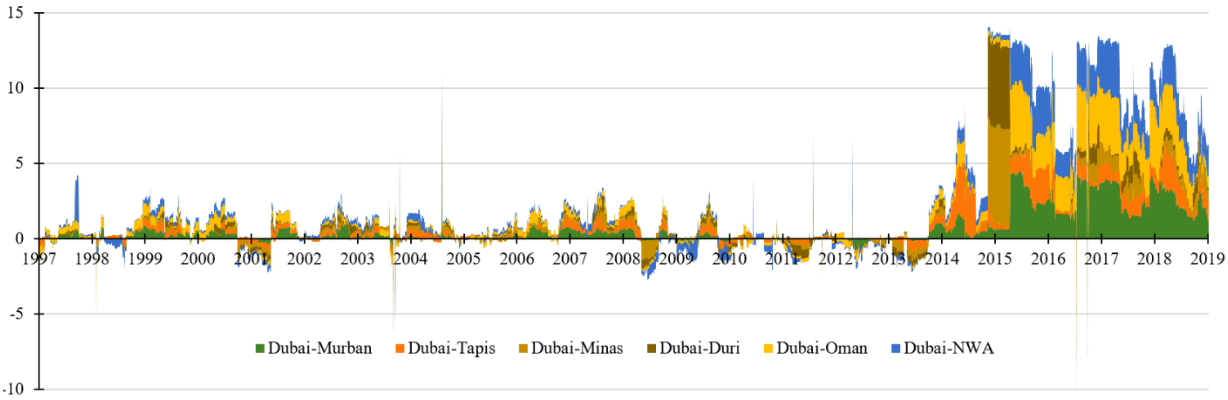

Figure 11: Aggregated net pairwise volatility spillovers between Dubai and regionals.

Moreover, in 2015 the TOCOM Crude futures changed to the Dubai benchmark as their sole underlying asset. This may have made the Dubai benchmark more closely knit to the Asian and Australian crudes through the activity of for instance hedgers and speculators utilizing the TOCOM Crude futures. In addition, the trade volume of TOCOM Crude futures significantly increased in 2015 due to for instance geopolitical unrest in the Middle East and global oversupply (TOCOM, 2016). The introduction of the Dubai benchmark as sole underlying asset to the TOCOM Crude futures may be the explanation of the rapid increase in net volatility spillover to Dubai from the regional crudes in 2015.

5.4 Analysis of WTI and Regionals

This part includes the empirical results from both the full-sample and rolling-window analysis of volatility spillover between WTI and regionals. The crudes included in this analysis are the benchmark WTI, and the regional crudes LLS, WTS and Alaskan. The regional crudes of this analysis are chosen to analyze the interaction between the U.S. domestic crudes as well as their effect on WTI in terms of volatility spillover. Both LLS and WTS cover the great oil producing regions in the south, while Alaskan covers the northern territory of the U.S.

5.4.1 Full-Sample Analysis of Volatility Spillover

The resulting total, directional and net spillovers from the full-sample analysis of volatility spillover between WTI and regionals are presented in Table 16. These results indicate that spillover effects account for about 65% of the volatility in each crude, i.e. high connectedness.

As observed from the diagonal elements, the own-variance share accounts for the majority of the volatility (around 35%) in the respective crudes. Both the volatility transmitted and received by all crude markets in this analysis is relatively equal for all the crudes (around 65%), and this may be due to the U.S. export ban which was active over the vast majority of the sample period. This may indicate that the export ban adequately served its purpose of isolating the U.S. market from global price volatility and the strategic pricing from OPEC (Langer et al., 2016).

Table 16: Volatility spillover table for WTI and regionals. Note: diagonal elements show own-variance shares, and off-diagonal elements show cross-variance shares. Directional FROM and TO others are estimated by equation (4.6) and (4.7), respectively. Total spillover index and net spillover are estimated by equation (4.5) and (4.8), respectively.

	WTI	**LLS**	**WTS**	**Alaskan**	**Directional FROM others**
WTI	34.32	21.51	20.54	23.63	65.68
LLS	21.71	36.27	22.26	19.76	63.73
WTS	21.23	22.86	36.45	19.45	63.54
Alaskan	24.97	19.92	19.27	35.84	64.16
Directional TO others	67.91	64.29	62.07	62.84	**Total spillover index:**
Directional including own	102.23	100.56	98.52	98.68	64.28 %
Net spillover	2.23	0.56	-1.47	-1.32	

As all markets both transmit and receive approximately equal amounts of volatility, the net spillover for all markets are relatively small. However, the net pairwise spillover table presented in Table 17 reveals information about the net direction of the spillovers. The results show that the benchmark WTI is a net transmitter of volatility to all the regional crudes included in this analysis. In contrast to the Brent benchmark, this observation may indicate that the WTI benchmark is relatively unaffected by its regional crudes.

Table 17: Net pairwise spillover table for WTI and regionals. The net pairwise spillovers are estimated by equation (4.9).

Net pairwise spillover				
	WTI	**LLS**	**WTS**	**Alaskan**
WTI	0	-0.20	-0.69	-1.34
LLS	0.20	0	-0.60	-0.16
WTS	0.69	0.60	0	0.18
Alaskan	1.34	0.16	-0.18	0

5.4.2 Rolling-Window Analysis of Volatility Spillover

In order to analyze the time-varying spillover effects, a rolling-window analysis of volatility spillover is conducted. The total volatility spillover index for WTI and its regionals is presented in Figure 12, and both a window of 100 and 250 days is utilized. As indicated in the results

from the full-sample analysis, the total volatility spillover index appears to be relatively stable around 60 and 70% across the entire sample. However, it is apparent from both panels that the connectedness experienced a severe drop from November 2012 to January 2015. This period was characterized by high and stable oil prices, as well as increasing U.S. oil production due to the fracking boom (ref. Figure 5).

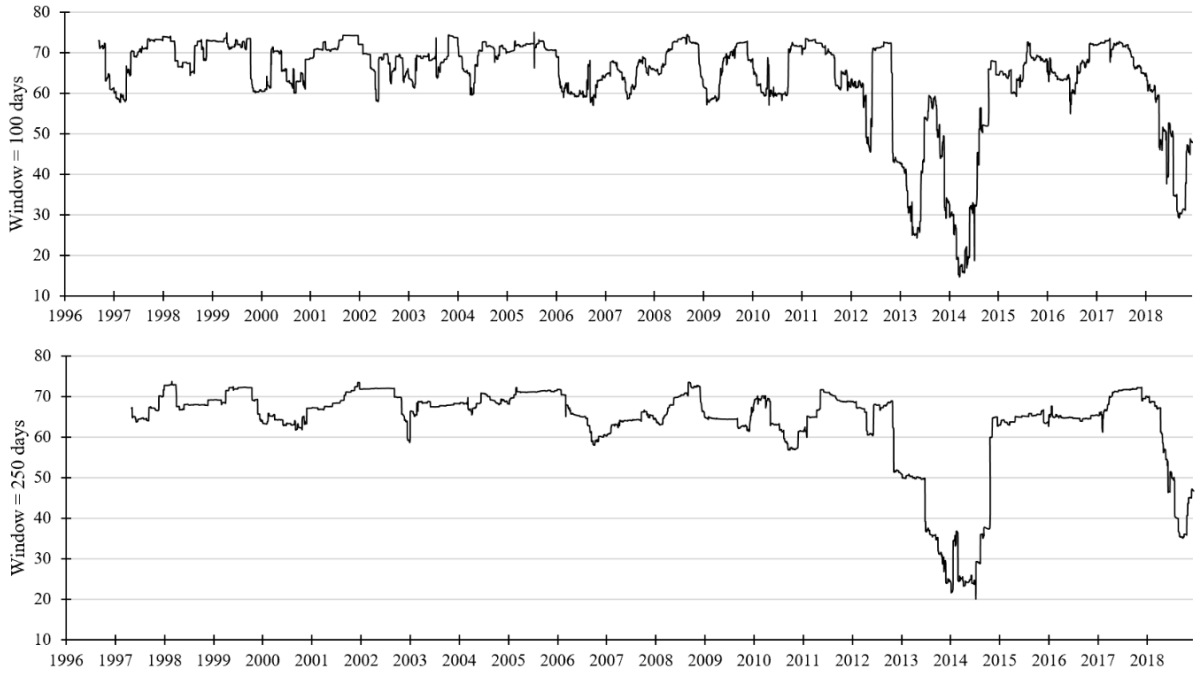

Figure 12: Total volatility spillover index for WTI and regionals.

In other words, the drop may be related to the U.S. shale oil revolution which is briefly described in terms of volatility spillover between benchmarks in subchapter 5.1.2. With this in mind, it is now necessary to take a closer look at how the U.S. shale oil revolution affected the American crude market internally. For starters, the U.S. refining industry was not well prepared for the rapid increase in domestic shale oil production. Before the fracking boom, the U.S. industry expected that the supply of light crudes would be increasingly scarce. In anticipation of this shift, the refineries located at the Gulf Coast and in Texas began restructuring to focus mainly on processing heavy crudes. At the same time, light crude refineries at the East Coast reduced their capacity. With the fracking boom, increasing quantities of light crudes were shipped to the market hub in Cushing, Oklahoma. Hence, the need for refining light crudes increased, but the restructuring process decreased the U.S. refining industry's capacity to refine such crudes. As already mentioned, the refineries capable of refining light crudes were located at the East Coast. However, adequate transportation infrastructure (pipelines) was not in place to ship oil from Cushing to the East Coast, nor to Texas. The alternative transportation mechanism was railroads, and as mentioned in subchapter 2.6.3, railroads are not capable of

moving the same amount of oil as pipelines. The lack of adequate transportation infrastructure in conjunction with the refinery restructuring process created a supply glut of light crudes in Cushing (Kilian, 2016).

According to Melek and Ojeda (2017), the supply glut in Cushing heavily penalized the WTI benchmark. For instance, WTI traded at a discount relative to LLS from 2011 to 2014 because LLS was not affected by the lack of adequate transportation infrastructure. The price spread between WTI and LLS during the U.S. shale oil revolution period is presented in Figure 13. The price spread between WTI and LLS is close to $20 during the entire period with a peak spread close to $30.

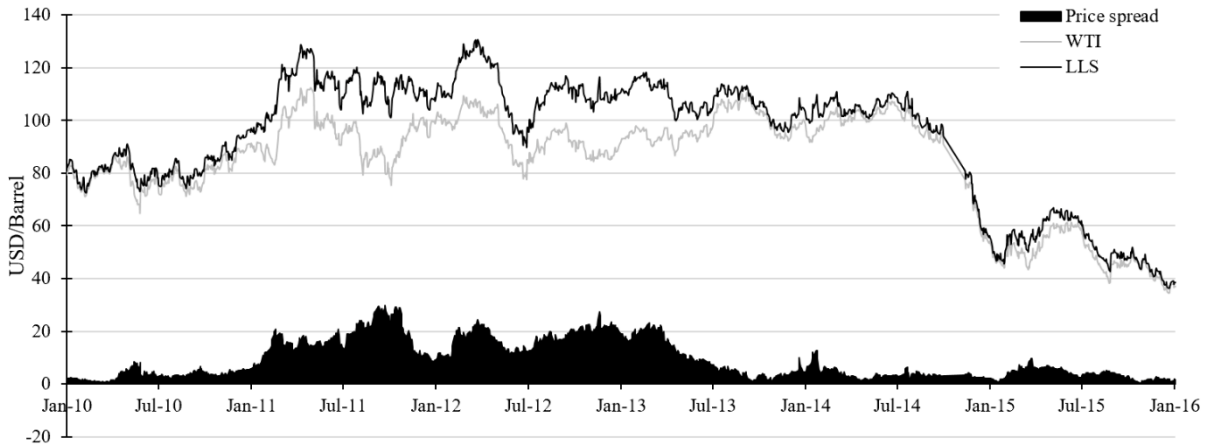

Figure 13: Price spread between WTI and LLS during the U.S. shale oil revolution.

A key thing to remember is that the U.S. crude oil export ban was active during this period, and not lifted until December 2015. The export ban exacerbated the domestic turmoil in the U.S. crude oil industry as the producers were unable to export the excess crude internationally (Melek and Ojeda, 2017). The U.S. transporting infrastructure began to improve in mid-2013 (Kilian, 2016), and finally when the export ban was lifted in 2015 both the price spread between WTI and LLS, and the drop in connectedness returned to normal conditions. All things considered, the drop in connectedness from November 2012 to January 2015 appears to be a series of unfortunate events occurring simultaneously, including the supply glut, lack of refining capacity, inadequate transportation infrastructure as well as the export ban.

To further understand the time-varying dynamics within the American crude oil market, it is interesting to analyze how the WTI benchmark interacts with the other American crude oils. In order to do so, the rolling net pairwise spillovers between WTI and its regionals are presented in Figure 14.

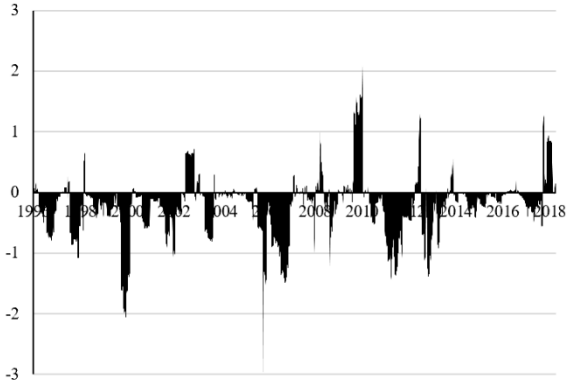

Panel A: From LLS to WTI

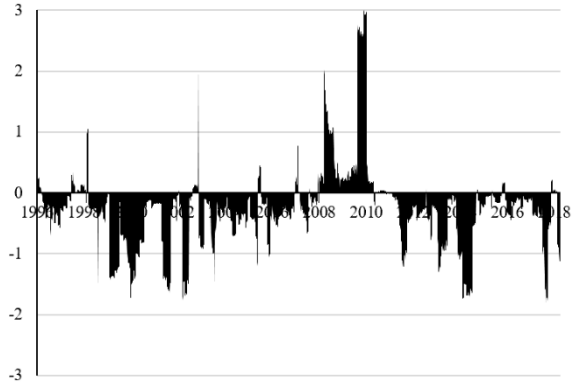

Panel B: From WTS to WTI

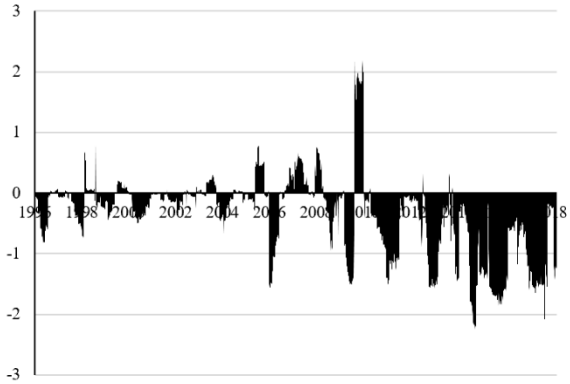

Panel C: From Alaskan to WTI

Figure 14: Net pairwise volatility spillovers between WTI and regionals.

As seen from the panels of Figure 14, there are small fluctuations in the net pairwise volatility spillovers between WTI and its regional crudes. It typically ranges between -2 and 0%, indicating that WTI is a marginal net transmitter of volatility to all the regional crudes over the entire sample period.

The behavior of the spillover between WTI and its regionals, both before and after the fracking boom started in 2011, is of particular interest. Up until 2011, when the fracking boom started, WTI was switching frequently between being net transmitter and net receiver of volatility. However, in the period after the fracking boom was initiated, WTI was almost exclusively a net transmitter to all American crudes considered in this thesis. Interestingly, this effect seems to be most significant for the Alaskan crude.

Above all, the findings from the rolling-window analysis further strengthens the hypothesis presented in the full-sample analysis that WTI is relatively unaffected by its regional crudes. As opposed to the Brent benchmark who receives volatility from its regional crudes, WTI is transmitting volatility to its regional crudes.

6 Conclusion

In this thesis, we have used daily spot prices for a set of 17 crude oils from May 1996 to January 2019 to analyze the volatility spillover between the three major benchmarks Brent, Dubai and WTI. Further, we have studied volatility spillover between each benchmark and its regional crudes. The regional crudes for each benchmark are chosen based on geographic vicinity and chemical similarities. In order to analyze the spillovers, we have utilized the generalized spillover index developed in Diebold and Yilmaz (2009; 2012). In general, our analyses suggest that the volatility spillover is time-varying, both in terms of strength and direction. In addition, we suggest that the time-varying uncertainty in the global crude oil market may be related to for instance global oil supply and demand, OPEC decisions, financial crises, national elections and geopolitical unrest.

Firstly, the results from the analysis of the benchmark crudes suggest moderate connectedness, where volatility spillover accounts for nearly a quarter of the volatility on average. The results further indicate that Dubai is the most significant contributor to uncertainty in the global crude oil market, and this is especially the case after the initiation of the Arab Spring. Furthermore, the spillover is time-varying and several peaks in connectedness can be identified throughout our sample period. Notably, we identified short-term spikes in connectedness which may have been related to the East Asian crisis, OPEC meetings, the Arab Spring, the U.S. fracking boom and the 2016 U.S. presidential election.

From the analysis of Brent and its regionals we find that almost three quarters of the volatility within the market is due to spillover effects. Our results further indicate that the connectedness is relatively stable within a range of 70 and 80%. However, the crudes experience a substantial drop in connectedness in 1998 which may have been related to the East Asian crisis. Furthermore, the results indicate that Brent is a net receiver of volatility from all the regional crudes. These findings suggest that the Brent benchmark behaves as a volatility buffer for the regional crudes. Interestingly, this is not only the case for the North Sea crudes, but also for the Russian and African crudes. This may be due to the chemical similarities of the Russian and African crudes compared to the benchmark.

Our analysis of Dubai and its regional crudes comprises a complex dataset, however we find a relatively high connectedness of about 50% between the crudes. Moreover, it seems to be a distinction between the Middle Eastern crudes and the Asian/Australian crudes in terms of their volatility spillover interactions with Dubai. The Middle Eastern crudes have the most

significant effect on Dubai in terms of uncertainty, furthermore we find that the effect appears to be decreasing, and changing direction, with geographical distance to Dubai. Our results also suggest that the Dubai benchmark became more connected to the Asian/Australian crudes after TOCOM changed to Dubai as their sole underlying asset in their Crude futures contracts.

We find that there is a high connectedness, about 65%, between WTI and its regional crudes. Further, we find that all crudes both transmit and receive equal amounts of uncertainty which may suggest that the U.S. export ban adequately served its purpose of isolating the U.S. market from global price volatility and the strategic pricing from OPEC. Moreover, it appears that most of the volatility spillover across our sample period may be primarily caused by a combination of imbalance in transportation and refining capacity, shale oil entry to the U.S. market, import and export of crudes. It appears that WTI experience opposite direction of the net volatility spillover to regional crudes compared to Brent. More specifically, our findings suggest that WTI is less affected by the pricing of its regional crudes compared to Brent.

Our study contributes to the discussion on market connectedness and volatility spillovers in crude oil markets. Furthermore, this thesis explores the volatility spillover dynamics between major crude oil benchmarks, and unlike most previous research in this area we also analyze the interdependence between major benchmarks and minor regional crudes as well as how these interrelationships vary across time. Understanding how crude oil markets are interrelated reveals important information to hedgers and speculators in the crude oil futures markets. Such knowledge is believed to be important, especially when developing hedging strategies and portfolio optimization through diversification. Further, we identify strength and direction of volatility spillover by utilizing the generalized spillover index developed in Diebold and Yilmaz (2009; 2012), and our findings are supported by market events which confirm that the methodology is well suited for this kind of analysis.

Finally, a key limitation of the current analysis is that the potential consequences of structural breaks in the underlying volatility series have not been taken into account. According to Jung and Maderitsch (2014), ignoring the importance of structural breaks may cause significant overestimation of volatility spillovers. The authors further state that after controlling for structural breaks, the volatility spillovers may be much weaker, or even disappear. To control for structural breaks, models such as the Markov switching model may be utilized. This methodology allows regime changes to occur in the underlying volatility series, and the results will therefore be robust to structural breaks (Lam, 2004). It would therefore be useful for future studies to utilize such models in the analysis.

7 References

ABDEL-AAL, H. K. & ALSAHLAWI, M. A. 2013. *Petroleum economics and engineering*, CRC Press.

ALBINALI, A. & DAHL, C. The Role of Hedging and Speculation in Recent Oil Price Formation Through Futures Markets. SPE Hydrocarbon Economics and Evaluation Symposium, 2014. Society of Petroleum Engineers.

ANDERSEN, T. G. & BOLLERSLEV, T. 1998. Answering the skeptics: Yes, standard volatility models do provide accurate forecasts. *International economic review*, 885-905.

ANDERSEN, T. G., BOLLERSLEV, T., DIEBOLD, F. X. & EBENS, H. 2001. The distribution of realized stock return volatility. *Journal of financial economics,* 61, 43-76.

AROURI, M. E. H., JOUINI, J. & NGUYEN, D. K. 2011. Volatility spillovers between oil prices and stock sector returns: Implications for portfolio management. *Journal of International money and finance,* 30, 1387-1405.

AWARTANI, B. & MAGHYEREH, A. I. 2013. Dynamic spillovers between oil and stock markets in the Gulf Cooperation Council Countries. *Energy Economics,* 36, 28-42.

BACHMEIER, L. J. & GRIFFIN, J. M. 2006. Testing for market integration crude oil, coal, and natural gas. *The Energy Journal*, 55-71.

BACON, R. & TORDO, S. 2005. Crude oil price differentials and differences in oil qualities: a statistical analysis.

BAEK, J. & SEO, J.-Y. 2015. A study on unobserved structural innovations of oil price: evidence from global stock, bond, foreign exchange, and energy markets. *Review of Pacific Basin Financial Markets Policies,* 18, 1550004.

BAHGAT, G. 2012. The impact of the Arab spring on the oil and gas industry in North Africa–a preliminary assessment. *The Journal of North African Studies,* 17, 503-514.

BARSKY, R. B. & KILIAN, L. 2004. Oil and the Macroeconomy since the 1970s. *Journal of Economic Perspectives,* 18, 115-134.

BARUNÍK, J., KOČENDA, E. & VÁCHA, L. 2015. Volatility spillovers across petroleum markets. *The Energy Journal*, 309-329.

BASEDAU, M. & RICHTER, T. 2014. Why do some oil exporters experience civil war but others do not?: investigating the conditional effects of oil. *European Political Science Review,* 6, 549-574.

BAUMEISTER, C. & KILIAN, L. 2016a. Forty years of oil price fluctuations: Why the price of oil may still surprise us. *Journal of Economic Perspectives,* 30, 139-60.

BAUMEISTER, C. & KILIAN, L. 2016b. Understanding the Decline in the Price of Oil since June 2014. *Journal of the Association of Environmental and Resource Economists,* 3, 131-158.

BAUMEISTER, C. & PEERSMAN, G. 2013. The role of time-varying price elasticities in accounting for volatility changes in the crude oil market. *Journal of Applied Econometrics,* 28, 1087-1109.

BBC. 2014. *Ukraine crisis: Timeline* [Online]. BBC. Available: https://www.bbc.com/news/world-middle-east-26248275 [Accessed 02.04.2019].

BEGG, S. H. & SMIT, N. Sensitivity of Project Economics to Uncertainty in Type and Parameters of Price Models. SPE Annual Technical Conference and Exhibition, 2007. Society of Petroleum Engineers.

BERK, J. B. & DEMARZO, P. M. 2007. Option Valuation. *Corporate Finance.* Pearson Education.

BHAR, R., HAMMOUDEH, S. & THOMPSON, M. A. 2008. Component structure for nonstationary time series: Application to benchmark oil prices. *International Review of Financial Analysis,* 17, 971-983.

BP. 2019. *Upstream* [Online]. BP. Available: https://www.bp.com/en/global/corporate/what-we-do/upstream.html [Accessed 22.03.2019].

BREITENFELLNER, A. & CUARESMA, J. C. 2008. Crude oil prices and the USD/EUR exchange rate. *Monetary Policy & The Economy*.

BROCKWELL, P. J., DAVIS, R. A. & CALDER, M. V. 2002. *Introduction to time series and forecasting*, Springer.

BU, H. 2014. Effect of inventory announcements on crude oil price volatility. *Energy Economics,* 46**,** 485-494.
BUIGUT, S. K. & VALEV, N. T. 2005. Is the proposed East African monetary union an optimal currency area? A structural vector autoregression analysis. *World Development,* 33**,** 2119-2133.
BÅRDSEN, G. & NYMOEN, R. 2014. *Videregående emner i Økonometri*, Fagbokforlaget Vigmostad Bjørke AS.
CANOVA, F. 2015. *Chapter 4: VAR models* [Online]. European University Institute. Available: http://apps.eui.eu/Personal/Canova/Articles/ch4.pdf [Accessed 11.02.2019].
CHANG, C.-L., LI, Y. & MCALEER, M. 2018. Volatility Spillovers between Energy and Agricultural Markets: A Critical Appraisal of Theory and Practice. *Energies,* 11**,** 1595.
CHATFIELD, C. 2016. *The analysis of time series: an introduction*, CRC press.
CHEVRON. 2019. *Operations* [Online]. Chevron. Available: https://www.chevron.com/operations [Accessed 22.03.2019].
CHIMA, C. M. & HILLS, D. 2007. Supply-chain management issues in the oil and gas industry. *Journal of Business & Economics Research,* 5**,** 27-36.
CINER, C., GURDGIEV, C. & LUCEY, B. M. 2013. Hedges and safe havens: An examination of stocks, bonds, gold, oil and exchange rates. *International Review of Financial Analysis,* 29**,** 202-211.
CUESTAS, J. C. & GIL-ALANA, L. A. 2018. Oil price shocks and unemployment in Central and Eastern Europe. *Ecnonmic Systems,* 42**,** 164-173.
DAHL, R. E. & JONSSON, E. 2018. Volatility spillover in seafood markets. *Journal of Commodity Markets,* 12**,** 44-59.
DAVIDSON, R. & MACKINNON, J. G. 2004. *Econometric theory and methods*, Oxford University Press New York.
DEMIRBAS, A., ALIDRISI, H. & BALUBAID, M. 2015. API gravity, sulfur content, and desulfurization of crude oil. *Petroleum Science Technology,* 33**,** 93-101.
DIEBOLD, F. X. & YILMAZ, K. 2009. Measuring financial asset return and volatility spillovers, with application to global equity markets. *The Economic Journal,* 119**,** 158-171.
DIEBOLD, F. X. & YILMAZ, K. 2012. Better to give than to receive: Predictive directional measurement of volatility spillovers. *International Journal of Forecasting,* 28**,** 57-66.
DIEBOLD, F. X. & YILMAZ, K. 2015. Trans-Atlantic equity volatility connectedness: US and European financial institutions, 2004–2014. 14**,** 81-127.
DU, X., CINDY, L. Y. & HAYES, D. 2011. Speculation and volatility spillover in the crude oil and agricultural commodity markets: A Bayesian analysis. *Energy Economics,* 33**,** 497-503.
EIA. 2019. *Petroleum & Other Liquids* [Online]. Available: https://www.eia.gov/dnav/pet/hist/LeafHandler.ashx?n=PET&s=WCRSTUS1&f=W [Accessed 27.02.2019].
ELLIOTT, G., ROTHENBERG, T. J. & STOCK, J. 1996. Efficient Tests for an Autoregressive Unit Root. *Econometrica,* 64**,** 813-36.
ENDERS, W. 2015. *Applied econometric time series*, John Wiley & Sons.
ENGLER, E. & NIELSEN, B. 2009. The empirical process of autoregressive residuals. *The Econometrics Journal,* 12**,** 367-381.
EQUINOR. 2019. *Corporate governance* [Online]. Equinor. Available: https://www.equinor.com/en/about-us/corporate-governance.html [Accessed 05.06.2019].
EVENSEN, D. 2016. US presidential candidates' views on unconventional gas and oil: Who has it right? *Energy research social science,* 20**,** 128-130.
FAHIM, M. A., AL-SAHHAF, T. A. & ELKILANI, A. 2009. *Fundamentals of petroleum refining*, Elsevier.
FATTOUH, B. 2006. The origins and evolution of the current international oil pricing system: A critical assessment. *In:* MABRO, R. (ed.) *Oil in the 21st century: Issues, challenges and Opportunities.* Oxford University Press.
FATTOUH, B. 2007. *OPEC pricing power: The need for a new perspective*, Oxford Institute for Energy Studies.
FATTOUH, B. 2010. The dynamics of crude oil price differentials. *Energy Economics,* 32**,** 334-342.

FATTOUH, B. 2011. *An anatomy of the crude oil pricing system*, Oxford Institute for Energy Studies.
FJAERTOFT, D. & OVERLAND, I. 2015. Financial sanctions impact Russian oil, equipment export ban's effects limited.
GAMBETTI, L. 2017. *2 Reduced Forms VARs* [Online]. Barcelona Gradue School of Economics. Available: http://pareto.uab.es/lgambetti/Lecture2M.pdf [Accessed 11.02.2019].
GARMAN, M. B. & KLASS, M. J. 1980. On the estimation of security price volatilities from historical data. *JOurnal of business***,** 67-78.
GEMAN, H. & OHANA, S. 2009. Forward curves, scarcity and price volatility in oil and natural gas markets. *Energy Economics,* 31**,** 576-585.
HAMILTON, J. D. 1983. Oil and the macroeconomy since World War II. *Journal of political economy,* 91**,** 228-248.
HAMILTON, J. D. 1996. This is what happened to the oil price-macroeconomy relationship. *Journal of Monetary Economics,* 38**,** 215-220.
HAMILTON, J. D. 2003. What is an oil shock? *Journal of Econometrics,* 113**,** 363-398.
HAMILTON, J. D. 2008. Understanding crude oil prices. National Bureau of Economic Research.
HAMILTON, J. D. 2009. Causes and Consequences of the Oil Shock of 2007-08. National Bureau of Economic Research.
HAMILTON, J. D. 2011. Historical oil shocks. National Bureau of Economic Research.
HEIJ, C., DE BOER, P., FRANSES, P. H., KLOEK, T. & VAN DIJK, H. K. 2004. *Econometric methods with applications in business and economics*, Oxford University Press.
HILYARD, J. 2012. *The oil & gas industry: A nontechnical guide*, PennWell Books.
HUDSON, J. 2013. *Phillips-Perron (PP) Unit Root Tests* [Online]. University of Bath. Available: http://staff.bath.ac.uk/hssjrh/Phillips%20Perron.pdf [Accessed 14.02.2019].
HURLEY, A., EGGLESTON, A., BUSHBY, D., CAMERON, D., FURNER, M., JOYCE, B., PRATT, L. & XENOPHON, N. 2008. Matters relating to the gas explosion at Varanus Islands, Western Australia. Parliament of Australia: Commonwealth of Australia.
HUSAIN, S., TIWARI, A. K., SOHAG, K. & SHAHBAZ, M. 2019. Connectedness among crude oil prices, stock index and metal prices: An application of network approach in the USA. *Resources Policy,* 62**,** 57-65.
INKPEN, A. C. & MOFFETT, M. H. 2011. *The global oil & gas industry: management, strategy & finance*, PennWell Books.
JAFARIZADEH, B. & BRATVOLD, R. 2013. Sell Spot or Sell Forward? Analysis of Oil-Trading Decisions With the Two-Factor Price Model and Simulation. *SPE Economics Management,* 5**,** 80-88.
JHAVERI, N. J. 2004. Petroimperialism: US oil interests and the Iraq War. *Antipode,* 36**,** 2-11.
JI, Q., BOURI, E., LAU, C. K. M. & ROUBAUD, D. 2018. Dynamic connectedness and integration in cryptocurrency markets. *International Review of Financial Analysis*.
JUNG, R. C. & MADERITSCH, R. 2014. Structural breaks in volatility spillovers between international financial markets: Contagion or mere interdependence? *Journal of Banking & Finance,* 47**,** 331-342.
KANG, S. H., KANG, S.-M. & YOON, S.-M. 2009. Forecasting volatility of crude oil markets. *Energy Economics,* 31**,** 119-125.
KANG, S. H., MCIVER, R. & YOON, S.-M. 2017. Dynamic spillover effects among crude oil, precious metal, and agricultural commodity futures markets. *Energy Economics,* 62**,** 19-32.
KARL, T. L. 1997. *The paradox of plenty: Oil booms and petro-states*, Univ of California Press.
KAUFMANN, R. K., DEES, S., KARADELOGLOU, P. & SANCHEZ, M. 2004. Does OPEC matter? An econometric analysis of oil prices. *The Energy Journal***,** 67-90.
KE, J., WANG, L. & MURRAY, L. 2010. An empirical analysis of the volatility spillover effect between primary stock markets abroad and China. *Journal of Chinese Economic and Business Studies,* 8**,** 315-333.
KENNEDY, P. 2003. *A guide to econometrics*, MIT press.
KILIAN, L. 2016. The impact of the shale oil revolution on US oil and gasoline prices. *Review of Environmental Economics Policy,* 10**,** 185-205.

KILIAN, L. & HICKS, B. 2013. Did unexpectedly strong economic growth cause the oil price shock of 2003–2008? *Journal of Forecasting,* 32**,** 385-394.
KILIAN, L. & PARK, C. 2009. The impact of oil price shocks on the US stock market. *International Economic Review,* 50**,** 1267-1287.
KILIAN, L. & VIGFUSSON, R. J. 2017. The role of oil price shocks in causing US recessions. *Journal of Money, Credit and Banking,* 49**,** 1747-1776.
KINZER, S. 2008. *All the Shah's men: An American coup and the roots of Middle East terror*, John Wiley & Sons.
KOOP, G., PESARAN, M. H. & POTTER, S. M. 1996. Impulse response analysis in nonlinear multivariate models. *Journal of Econometrics,* 74**,** 119-147.
KREHLIK, T. 2018. Package 'frequencyConnectedness'. *Spectral Decomposition of Connectedness Measures.*
LAM, P. S. 2004. A Markov-switching model of Gnp growth with duration dependence. *International Economic Review,* 45**,** 175-204.
LANGER, L., HUPPMANN, D. & HOLZ, F. 2016. Lifting the US crude oil export ban: A numerical partial equilibrium analysis. *Energy Policy,* 97**,** 258-266.
LE BILLON, P. 2001. Angola's political economy of war: The role of oil and diamonds, 1975–2000. *African Affairs,* 100**,** 55-80.
LERAAND, D. 2017. *Den Arabiske Våren* [Online]. Store Norske Leksikon. Available: https://snl.no/Den_arabiske_våren [Accessed 01.04.2019].
LÜTKEPOHL, H. 2005. *New introduction to multiple time series analysis*, Springer Science & Business Media.
MALIK, F. & HAMMOUDEH, S. 2007. Shock and volatility transmission in the oil, US and Gulf equity markets. *International Review of Economics Finance,* 16**,** 357-368.
MARTÍNEZ-PALOU, R., DE LOURDES MOSQUEIRA, M., ZAPATA-RENDÓN, B., MAR-JUÁREZ, E., BERNAL-HUICOCHEA, C., DE LA CRUZ CLAVEL-LÓPEZ, J. & ABURTO, J. 2011. Transportation of heavy and extra-heavy crude oil by pipeline: A review. *Journal of Petroleum Science and Engineering,* 75**,** 274-282.
MCKINSEY. 2019. *API gravity* [Online]. Energy Insights By McKinsey. Available: https://www.mckinseyenergyinsights.com/resources/refinery-reference-desk/api-gravity/ [Accessed 19.02.2019].
MELEK, N. Ç. & OJEDA, E. 2017. Lifting the US Crude Oil Export Ban: Prospects for Increasing Oil Market Efficiency. *Economic Review-Federal Reserve Bank of Kansas City,* 102**,** 51-74.
MERIEM-BENZIANE, M., BOU-SAÏD, B. & BOUDOUANI, N. 2017. The effect of crude oil in the pipeline corrosion by the naphthenic acid and the sulfur: A numerical approach. *Journal of Petroleum Science and Engineering,* 158**,** 672-679.
NARAYAN, P. K. & NARAYAN, S. 2007. Modelling oil price volatility. *Energy Policy,* 35**,** 6549-6553.
NAZLIOGLU, S., ERDEM, C. & SOYTAS, U. 2013. Volatility spillover between oil and agricultural commodity markets. *Energy Economics,* 36**,** 658-665.
PATTON, A. J. 2011. Volatility forecast comparison using imperfect volatility proxies. *Journal of Econometrics,* 160**,** 246-256.
PESARAN, H. H. & SHIN, Y. 1998. Generalized impulse response analysis in linear multivariate models. *Economics letters,* 58**,** 17-29.
PFAFF, B. & STIGLER, M. 2018. Package 'vars'. *VAR Modelling.*
PHAN, D. H. B., TRAN, V. T. & NGUYEN, D. T. 2018. Crude oil price uncertainty and corporate investment: New global evidence. *Energy Economics*.
PINDYCK, R. S. 1990. Inventories and the short-run dynamics of commodity prices. National Bureau of Economic Research.
PINDYCK, R. S. 2001. The dynamics of commodity spot and futures markets: a primer. *The energy journal***,** 1-29.
PINDYCK, R. S. 2004a. Volatility and commodity price dynamics. *Journal of Futures Markets: Futures, Options, and Other Derivative Products,* 24**,** 1029-1047.

PINDYCK, R. S. 2004b. Volatility in natural gas and oil markets. *The Journal of Energy Development,* 30**,** 1-19.
PLANTE, M. 2019. OPEC in the News. *Energy Economics,* 80**,** 163-172.
POON, S.-H. & GRANGER, C. 2005. Practical issues in forecasting volatility. *Financial Analysts Journal***,** 45-56.
PUTNAM, B. & BRUSSTAR, D. 2015. U.S. Crude oil export ban lifted. *CME Group*.
R-PROJECT. 2019. *What is R?* [Online]. The R Foundation. Available: https://www.r-project.org/about.html [Accessed 13.03.2019].
RAD, J. A., HÖÖK, J., LARSSON, E. & VON SYDOW, L. 2018. Forward deterministic pricing of options using Gaussian radial basis functions. *JOurnal of Computational Science,* 24**,** 209-217.
RAKKESTAD, K. J. 2002. *Estimering av indikatorer for volatilitet*, Norges Bank.
REALCLEARPOLITICS. 2016. *General Election: Trump vs. Clinton* [Online]. Available: https://www.realclearpolitics.com/epolls/2016/president/us/general_election_trump_vs_clinton-5491.html [Accessed 03.04.2019].
ROSS, M. L. 2004. What do we know about natural resources and civil war? *Journal of peace research,* 41**,** 337-356.
ROSS, S., WESTERFIELD, R., JAFFE, J. & JORDAN, B. 2018. *Corporate Finance: Core Principles & Applications*, McGraw Hill.
RUSTAD, S. A. & BINNINGSBØ, H. M. 2012. A price worth fighting for? Natural resources and conflict recurrence. *Journal of Peace Research,* 49**,** 531-546.
SCHMIDBAUER, H. & RÖSCH, A. 2012. OPEC news announcements: Effects on oil price expectation and volatility. *Energy Economics,* 34**,** 1656-1663.
SCHWAGER, J. D. & ETZKORN, M. 2017. *A complete guide to the futures markets: fundamental analysis, technical analysis, trading, spreads, and options*, John Wiley & Sons.
SHELL. 2019. *Dette gjør vi* [Online]. Shell. Available: https://www.shell.no/about-us/what-we-do.html [Accessed 22.03.2019].
SHU, J. & ZHANG, J. E. 2006. Testing range estimators of historical volatility. *Journal of Futures Markets,* 26**,** 297-313.
SIEMINSKI, A. 2014. Implications of the US shale revolution. *Presentation at the US–Canada Energy Summit*.
SINGH, V. K., KUMAR, P. & NISHANT, S. 2019. Feedback Spillover Dynamics of Crude Oil and Global Assets Indicators: A System-wide Network Perspective. *Energy Economics*.
SPEIGHT, J. G. 2015. *Handbook of petroleum product analysis*, John Wiley & Sons.
SPEIGHT, J. G. 2017. *Rules of Thumb for Petroleum Engineers*, John Wiley & Sons.
STEVENS, P. 2012. *The Arab uprisings and the international oil markets*, Citeseer.
STOCK, J. H. & WATSON, M. W. 2012. *Introduction to econometrics*, Pearson.
STOCK, J. H. J. H. O. E. 1994. Unit roots, structural breaks and trends. 4**,** 2739-2841.
TOCOM. 2016. *TOCOM Dubai Crude Oil* [Online]. TOCOM. Available: https://www.tocom.or.jp/dubaicrude/ [Accessed 10.05.2019].
TOMEK, W. G. & KAISER, H. M. 2014. *Agricultural product prices*, Cornell University Press.
TOTAL. 2019. *Our expertise* [Online]. Total. Available: https://www.total.com/en/energy-expertise [Accessed 22.03.2019].
VAN VACTOR, S. 2010. *Introduction to the global oil & gas business*, PennWell Books.
WALPOLE, R. E., MYERS, R. H., MYERS, S. L. & YE, K. 2016. *Probability & Statistics for Engineers & Scientists*, Pearson Education.
WANG, G., SPENCER, J. & ELSAYED, T. Estimation of corrosion rates of structural members in oil tankers. Proceedings of OMAE, 2003.
WEI, Y., LIU, J., LAI, X. & HU, Y. 2017. Which determinant is the most informative in forecasting crude oil market volatility: Fundamental, speculation, or uncertainty? *Energy Economics,* 68**,** 141-150.
WOOLDRIDGE, J. M. 2015. *Introductory econometrics: A modern approach*, Nelson Education.

ZAVADSKA, M., MORALES, L. & COUGHLAN, J. 2018. Brent crude oil prices volatility during major crises. *Finance Research Letters*.

ZHANG, D. 2017. Oil shocks and stock markets revisited: measuring connectedness from a global perspective. *Energy Economics,* 62**,** 323-333.

ØGLEND, A. 2018. Commodity Price Variation and Price Risk Hedging. *In:* A COMPENDIUM TO IND 640 - RISK, D. A. M. (ed.). University of Stavanger.